INVITED SURVEY PAPER

Introduction of Frequency-Domain Signal Processing to Broadband Single-Carrier Transmissions in a Wireless Channel

Fumiyuki ADACHI[†a)], ***Fellow***, **Hiromichi TOMEBA**[†], ***and*** **Kazuki TAKEDA**[†], ***Student Members***

SUMMARY Recently, frequency-domain equalization (FDE) has been attracting much attention as a way to improve single-carrier (SC) signal transmission in a frequency-selective wireless channel. Since the SC signal spectrum is spread over the entire signal bandwidth, FDE can take advantage of channel frequency-selectivity and achieve the frequency diversity gain. SC with FDE is a promising wireless signal transmission technique. In this article, we review the pioneering research done on SC with FDE. The principles of simple one-tap FDE, channel estimation, and residual inter-symbol interference (ISI) cancellation are presented. Multi-input/multi-output (MIMO) is an important technique to improve the transmission performance. Some of the studies on MIMO/SC with FDE are introduced.

key words: *single-carrier, frequency-domain equalization, frequency-selective channel, wireless systems*

1. Introduction

Public cellular mobile communications services started about 30 years ago with so called 1st generation (1G) systems using analog wireless technology. In line with the recent explosive expansion of Internet traffic in the fixed networks, demands for broad ranges of data communications services are becoming stronger even in cellular mobile communications systems. A variety of data communications services are now available over the 2nd/3rd generation (2G/3G) systems using digital wireless technology. The 3G systems using direct-sequence code division multiple access (DS-CDMA) technique [1], with much higher data rates up to 384 kbps than 2G systems, have already been deployed in many countries. 3G systems are continuously evolving with high speed downlink packet access (HSDPA) technique for providing data services with the peak rate of around 14 Mbps as the mid-term evolution and of 50–100 Mbps as the long-term evolution (LTE) [2]. However, the capabilities of 3G systems will sooner or later be insufficient to cope with the increasing demands for broadband services. The 3G-LTE systems will be followed by the development of 4th generation (4G) systems, that support broadband data services with the peak rate of e.g., 100 M–1 Gbps [3].

The propagation channel for broadband wireless communications comprises many distinct paths resulting from reflection and diffraction due to many obstacles located between a transmitter and a receiver. Therefore, the channel transfer function, $H(f, t)$, varies both in the frequency domain, f, and time domain, t. Figure 1 illustrates a one shot observation of $H(f, t)$. This type of channel is called the frequency- and time-selective channel (or doubly selective channel). In such a frequency-selective channel, the received signal spectrum is severely distorted [4]. Thus, the use of data transmission technique with an advanced equalization technique is indispensable in 3G-LTE and 4G systems.

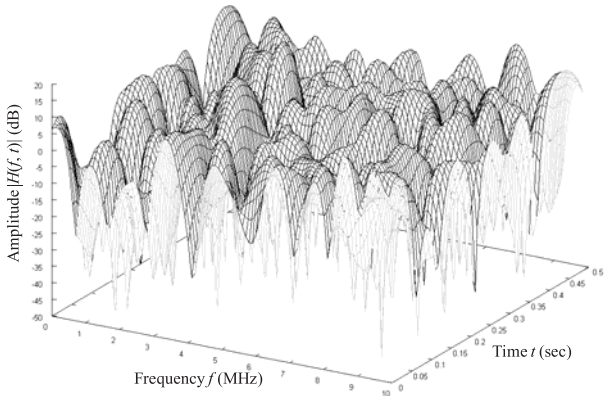

Fig. 1 Frequency- and time-selective channel. L = 16-path uniform power delay profile with delay time separation of 100 ns.

Single-carrier (SC) signal transmission technique, such as DS-CDMA with coherent rake combining used in the present 3G systems [1], provides very poor performance because of strong inter-chip interference (ICI) resulting from severe frequency-selectivity of the channel. Therefore, multi-carrier CDMA (MC-CDMA) with frequency-domain equalization (FDE) [5]–[7] has long been considered as a broadband multiple access technique since it can take advantage of channel frequency-selectivity to improve the transmission performance. Special cases of DS-CDMA and MC-CDMA are non-spread SC multiple access and orthogonal frequency division multiple access (OFDMA), respectively. However, it was shown by many researchers that SC transmission performance in a frequency-selective channel can be significantly improved by the use of low-complexity FDE [8]–[13]. An advantage of SC signal transmission technique over MC signal transmission technique is its lower peak-to-average power ratio (PAPR). This lower PAPR property of SC is quite beneficial for the application to the uplink (mobile-to-base) transmissions. In 3G-LTE

Manuscript received September 17, 2008.
Manuscript revised February 22, 2009.

[†]The authors are with the Department of Electrical and Communication Engineering, Graduate School of Engineering, Tohoku University, Sendai-shi, 980-8579 Japan.
a) E-mail: adachi@ecei.tohoku.ac.jp

DOI: 10.1587/transcom.E92.B.2789

systems, different multiple access techniques are adopted for the downlink (base-to-mobile) and the uplink first time in the mobile communications history; the downlink access uses OFDMA and the uplink access uses so-called SC-FDMA, which is a combination of SC with FDE and frequency division multiple access (FDMA) [14].

In this article, we review the pioneering research done on SC with FDE. After modeling the mobile channel in Sect. 2, Sect. 3 presents a literature survey of the time-domain and frequency-domain equalization techniques for SC signal transmission. Section 4 overviews the FDE technique. The principle of simple one-tap FDE is presented, and the channel capacity that can be achieved by one-tap FDE is discussed. Section 5 introduces overlap FDE technique to further improve the transmission efficiency. Also introduced is fractionally spaced FDE. The performance improvement through the use of FDE is limited by the presence of residual inter-symbol interference (ISI). An interference cancellation technique can be used to eliminate the residual ISI. This is described in Sect. 6. FDE requires channel state information in order to obtain the equalization weight. Some studies on channel estimation are reviewed in Sect. 7. The multi-input/multi-output (MIMO) antenna technique plays an important role in future wireless systems. Section 8 introduces recent studies on MIMO/SC with FDE. MIMO diversity, array, and spatial multiplexing techniques are also discussed. FDE can be applied to transmitters to alleviate the complexity problem of mobile terminals. Section 9 reviews the pre-FDE technique. Section 10 concludes the paper.

2. Broadband Wireless Channel Model

Assuming that the channel comprises L paths, the channel impulse response, $h(\tau)$, can be expressed as [15]

$$h(\tau) = \sum_{l=0}^{L-1} h_l \delta(\tau - \tau_l), \tag{1}$$

where h_l and τ_l are the complex-valued path gain with $E\left[\sum_{l=0}^{L-1} |h_l|^2\right] = 1$ ($E[.]$ denotes the expectation operation) and the symbol-spaced time delay of the lth path, respectively. In Eq. (1), we assumed that the channel stays constant during the signal transmission period of interest; therefore, time dependency has been omitted from Eq. (1). The channel transfer function (or the channel gain at frequency f) is given by

$$H(f) = \sum_{l=0}^{L-1} h_l \exp(-j2\pi f \tau_l). \tag{2}$$

The transmit signal is denoted by $s(t)$ with $E\left[|s(t)|^2\right] = 1$. The received signal, $r(t)$, at time t can be expressed using the baseband equivalent representation as

$$r(t) = \sqrt{\frac{2E_s}{T_s}} \sum_{l=0}^{L-1} h_l s(t - \tau_l) + n(t), \tag{3}$$

where E_s and T_s are the data symbol energy and time duration, respectively, and $n(t)$ is a zero-mean complex-valued additive white Gaussian noise (AWGN) with variance $2N_0/T_s$ (N_0 is the one-sided power spectrum density). $L-1$ past signals $\{s(t-\tau_l); l = 1 \sim (L-1)\}$ interfere with the present signal, $s(t)$, thereby producing the ISI. As L increases, the channel frequency-selectivity level increases and the ISI becomes increasingly worse. As the signal transmission rate increases, the symbol time length becomes shorter and therefore, the number of resolvable propagation paths increases. Some equalization techniques to eliminate the ISI must be developed in order to improve the transmission performance.

3. Literature Survey

The development history of time-domain decision feedback equalization (DFE) (or ISI cancellation) techniques is overviewed in [16]. The idea that the previous decisions are used to cope with the ISI problem was first introduced in [17] and was later extended in [18] to minimize the mean square error (MSE) between the decision variable and the transmitted symbol. The optimum equalizer assuming ideal decision feedback is a matched filter to the channel [18]. The optimum DFE technique was derived in [19] and [20]. An iterative equalization technique proposed in [21] provides a performance level that approaches the maximum likelihood sequence detection (MLSD) in a severe ISI channel.

Time-domain nonlinear DFE is used to eliminate the ISI. On the other hand, linear frequency-domain equalization (FDE) can be used to take advantage of the frequency-selective channel, while it has a lower computational complexity level than that for the time-domain DFE. The first application of FDE to SC transmission can be found in [8] and [9]. An overview of SC with FDE can be found in [11].

A striking resemblance exists between SC with FDE and OFDM. The only difference is that in OFDM, both channel equalization and decision making are performed in the frequency-domain, whereas in SC with FDE, the channel equalization is performed in the frequency-domain and decisions are made in the time-domain. SC with FDE has the advantage of low sensitivity to nonlinear signal distortion and can alleviate the carrier synchronization problem of OFDM [11]. In [10], a performance comparison is presented between OFDM and SC with FDE. A major advantage of SC with FDE compared to OFDM is that since the energy of each data symbol is spread over the whole frequency range, narrowband notches in the channel transfer function have only a small impact on the decision error probability. As a consequence, SC with FDE outperforms OFDM with respect to the bit error rate (BER) performance when no channel coding is employed.

The FDE weight can be based on the zero-forcing (ZF) criterion or the minimum mean square error (MMSE) criterion. ZF-FDE restores the original spectrum regardless of the channel conditions, but enhances the noise power

after equalization. On the other hand, MMSE-FDE gives up the restoration of original signal spectrum, but it minimizes the power sum of the residual ISI and additive noise after the equalization. The lower PAPR is also an important advantage of SC with FDE, whereas a major advantage of OFDM is that the use of the subcarrier-by-subcarrier adaptive modulation scheme can significantly improve the BER performance. SC with FDE outperforms OFDM with respect to the sensitivity to power amplifier nonlinearities and frequency offsets [10].

Although MMSE-FDE can significantly improve the BER performance of SC transmission compared to ZF-FDE, a big performance gap still exists from the theoretical lower bound (or the matched filter bound). This is due to the presence of residual ISI after MMSE-FDE. A combination of FDE and DFE for eliminating the residual ISI is an interesting study topic. In [11], not only the basic concept of SC with FDE but also advanced FDE jointly using DFE is introduced. In the DFE technique proposed in [22], the feedforward part is implemented in the frequency-domain, while a feedback signal is generated using time-domain filtering. The application of frequency-domain DFE to the SC transmission is found in [23]. In [24] and [25], an iterative block DFE, which redesigns the equalizer based on the updated block of detected symbols, is presented. Both feedforward and feedback filters are implemented using FFTs to achieve a significant complexity reduction compared to time-domain techniques.

The structure of iterative FDE using decision feedback is compatible with error-control coding. It may be possible to combine a turbo-style decoder and iterative FDE into a single efficient equalizer-decoder structure comparable to the class of "turbo equalization" [26].

The application of FDE to DS-CDMA system was discussed in [12] and [13]. DS-CDMA with FDE can take advantage of the channel frequency-selectivity and achieve the frequency diversity gain to improve the BER performance while the FDE complexity level is kept much lower than that for time-domain equalization and does not change significantly with the length of the channel impulse response. In [13], broadband wireless access techniques such as MC-CDMA and DS-CDMA using MMSE-FDE are compared. Most data services provided in the next generation wireless communication systems will be broadband packet based. FDE can be combined with hybrid automatic repeat request (HARQ).

4. Frequency-Domain Equalization (FDE)

First, the principle of one-tap FDE for SC signal transmissions is presented. Then, the channel capacity achievable with one-tap FDE in a frequency-selective Rayleigh fading channel is discussed. From now onward, we use the discrete-time signal representation with variable t (= $0 \sim (N_c - 1)$) representing the symbol-spaced discrete time and τ_l representing the lth path time delay normalized by the symbol length, T_s.

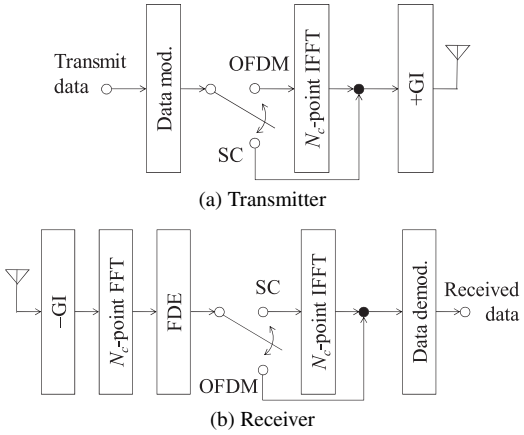

Fig. 2 Transmitter/receiver structure for SC and OFDM. "+GI" and "−GI" represent the insertion and removal of the GI, respectively.

4.1 Principle of One-Tap FDE

Figure 2 illustrates the transmitter/receiver structure for SC with FDE and OFDM. The difference between SC with FDE and OFDM is the location of the inverse fast Fourier transform (IFFT) function. The IFFT is required at the transmitter for OFDM, while it is required at the receiver for SC. This allows a flexible transceiver architecture based on software-defined radio technology, which can flexibly switch between SC and OFDM.

Both SC with FDE and OFDM are a block transmission. Below, we consider the transmission of one block of N_c symbols.

For OFDM signal transmission, N_c-point IFFT is applied to an N_c-symbol block $\{s(t);\ t = 0 \sim (N_c - 1)\}$ to generate the time-domain OFDM signal waveform with N_c subcarriers. In SC signal transmission, however, no IFFT is required. Similar to OFDM signal transmission, the guard interval (GI) of N_g samples is inserted in front of each N_c-symbol block to avoid the inter-block interference (IBI) from the previous block. The GI length should be longer than the maximum time delay difference among the propagation paths.

An N_c-symbol block is transmitted after inserting an N_g-symbol cyclic prefix (CP) into the GI so that the received signal can be a circular convolution of the transmitted signal block and the channel impulse response. The received SC signal is expressed as Eq. (3). Due to the CP insertion into the GI, Eq. (3) can be rewritten, for $t = 0 \sim (N_c - 1)$, as

$$r(t) = \sqrt{\frac{2E_s}{T_s}} \sum_{l=0}^{L-1} h_l s((t - \tau_l) \bmod N_c) + n(t). \tag{4}$$

Note that, after the GI insertion, T_s is shorter by a factor of $(1 + N_g/N_c)$ than the original data symbol length or the signal bandwidth is wider by a factor of $(1 + N_g/N_c)$ than the original signal bandwidth.

The received symbol block after removing the GI can be expressed in the matrix form as

$$\begin{aligned}\boldsymbol{r} &= [r(0), \cdots, r(t), \cdots, r(N_c-1)]^T \\ &= \sqrt{\frac{2E_s}{T_s}}\boldsymbol{h}\boldsymbol{s} + \boldsymbol{n}, \end{aligned} \tag{5}$$

where $[.]^T$ denotes the transpose operation, $\boldsymbol{s} = [s(0), \cdots, s(t), \cdots, s(N_c-1)]^T$ is the time-domain transmit signal vector, $\boldsymbol{n} = [n(0), \cdots, n(t), \cdots, n(N_c-1)]^T$ is the noise vector, and $\boldsymbol{h}$ is the circulant channel impulse response matrix, given by

$$\boldsymbol{h} = \begin{bmatrix} h_0 & & & & h_{L-1} & \cdots & h_1 \\ h_1 & \ddots & & & & \ddots & \vdots \\ \vdots & \ddots & h_0 & & \mathbf{0} & & h_{L-1} \\ h_{L-1} & & h_1 & \ddots & & & \\ & \ddots & \vdots & \ddots & \ddots & & \\ & & h_{L-1} & & \ddots & h_0 & \\ & & & \ddots & & h_1 & \ddots \\ \mathbf{0} & & & & \ddots & \vdots & \ddots & h_0 \end{bmatrix}. \tag{6}$$

At the receiver, the received signal block is transformed using the N_c-point FFT into the frequency-domain signal. The frequency-domain received signal vector, $\boldsymbol{R} = [R(0), \cdots, R(k), \cdots, R(N_c-1)]^T$, can be expressed as

$$\boldsymbol{R} = \boldsymbol{F}\boldsymbol{r} = \sqrt{\frac{2E_s}{T_s}}\boldsymbol{H}\boldsymbol{S} + \boldsymbol{N}, \tag{7}$$

where $\boldsymbol{F}$ is an $N_c \times N_c$ FFT matrix, $\boldsymbol{S} = \boldsymbol{F}\boldsymbol{s} = [S(0), \cdots, S(k), \cdots, S(N_c-1)]^T$ is the frequency-domain transmit signal vector, and $\boldsymbol{N} = \boldsymbol{F}\boldsymbol{n} = [N(0), \cdots, N(k), \cdots, N(N_c-1)]^T$ is the frequency-domain noise vector. The $N_c \times N_c$ channel matrix, $\boldsymbol{H} = \boldsymbol{F}\boldsymbol{h}\boldsymbol{F}^H$, becomes diagonal because of the circulant property of $\boldsymbol{h}$ and is given by

$$\boldsymbol{H} = \boldsymbol{F}\boldsymbol{h}\boldsymbol{F}^H = \begin{bmatrix} H(0) & & & \\ & \ddots & \mathbf{0} & \\ & & H(k) & \\ & \mathbf{0} & & \ddots \\ & & & H(N_c-1) \end{bmatrix}, \tag{8}$$

where $[.]^H$ denotes the Hermitian transpose operation. The k-th element, $R(k)$, of $\boldsymbol{R}$ can be expressed as

$$R(k) = \sqrt{\frac{2E_s}{T_s}}H(k)S(k) + N(k), \tag{9}$$

where $H(k)$, $S(k)$, and $N(k)$ are the channel gain, the transmit signal component, and the noise component at the k-th frequency, respectively, and are given by

$$\begin{cases} H(k) = \displaystyle\sum_{l=0}^{L-1} h_l \exp\left(-j2\pi k\frac{\tau_l}{N_c}\right) \\ S(k) = \dfrac{1}{\sqrt{N_c}} \displaystyle\sum_{t=0}^{N_c-1} s(t)\exp\left(-j2\pi k\frac{t}{N_c}\right) \\ N(k) = \dfrac{1}{\sqrt{N_c}} \displaystyle\sum_{t=0}^{N_c-1} n(t)\exp\left(-j2\pi k\frac{t}{N_c}\right) \end{cases}. \tag{10}$$

One-tap FDE is carried out as

$$\hat{R}(k) = W(k)R(k) \tag{11}$$

where $W(k)$ is the FDE weight. Various FDE weights exist such as those based on ZF, equal-gain combining (EGC), maximal-ratio combining (MRC), and MMSE criteria. They are given as

$$W(k) = \begin{cases} 1/H(k), & \text{ZF} \\ H^*(k)/|H(k)|, & \text{EGC} \\ H^*(k), & \text{MRC} \\ \dfrac{H^*(k)}{|H(k)|^2 + (E_s/N_0)^{-1}}, & \text{MMSE} \end{cases}. \tag{12}$$

Using $N_c \times N_c$ FDE weight matrix $\boldsymbol{W} = \text{diag}\{W(0), \cdots, W(k), \cdots, W(N_c-1)\}$ and $\boldsymbol{S} = \boldsymbol{F}\boldsymbol{s}$, the frequency-domain received signal vector, $\hat{\boldsymbol{R}} = [\hat{R}(0), \cdots, \hat{R}(k), \cdots, \hat{R}(N_c-1)]^T$, after FDE can be expressed as

$$\hat{\boldsymbol{R}} = \boldsymbol{W}\boldsymbol{R} = \sqrt{\frac{2E_s}{T_s}}\hat{\boldsymbol{H}}\boldsymbol{F}\boldsymbol{s} + \boldsymbol{W}\boldsymbol{N}, \tag{13}$$

where

$$\hat{\boldsymbol{H}} = \text{diag}\{\hat{H}(0), \cdots, \hat{H}(k), \cdots, \hat{H}(N_c-1)\} = \boldsymbol{W}\boldsymbol{H} \tag{14}$$

is the equivalent channel matrix with $\hat{H}(k) = W(k)H(k)$.

Since the frequency-nonselective channel has a constant channel gain over all k, the signal received via a frequency-nonselective channel is a scaled version of the transmitted signal $s(t)$ and no ISI is present. The equivalent channel $\hat{\boldsymbol{H}}$ can be divided into two parts as

$$\hat{\boldsymbol{H}} = A \cdot \boldsymbol{I} + \left(\hat{\boldsymbol{H}} - A \cdot \boldsymbol{I}\right), \tag{15}$$

where the first term represents a frequency-nonselective channel in $\hat{\boldsymbol{H}}$ and A is the average equivalent channel gain after FDE, defined as

$$A = \frac{1}{N_c}\sum_{k=0}^{N_c-1}\hat{H}(k). \tag{16}$$

As a consequence, the frequency-domain received signal vector $\hat{\boldsymbol{R}}$ after FDE can be rewritten as

$$\hat{\boldsymbol{R}} = \sqrt{\frac{2E_s}{T_s}}A \cdot \boldsymbol{F}\boldsymbol{s} + \boldsymbol{M} + \boldsymbol{W}\boldsymbol{N}, \tag{17}$$

where $\boldsymbol{M} = [M(0), \cdots, M(k), \cdots, M(N_c-1)]^T$ is the residual ISI vector. $\boldsymbol{M}$ is given as

$$\boldsymbol{M} = \sqrt{\frac{2E_s}{T_s}}\left\{\hat{\boldsymbol{H}} - A \cdot \boldsymbol{I}\right\}\boldsymbol{F}\boldsymbol{s}, \tag{18}$$

where

$$M(k) = \sqrt{\frac{2E_s}{T_s}}\left\{\hat{H}(k) - A\right\}S(k). \tag{19}$$

For SC with FDE, the estimate $\hat{\boldsymbol{s}} = [\hat{s}(0), \cdots, \hat{s}(t), \cdots, \hat{s}(N_c-1)]^T$ of the transmitted symbol vector $\boldsymbol{s}$ is obtained by applying N_c-point IFFT to $\hat{\boldsymbol{R}}$, while it is not required for

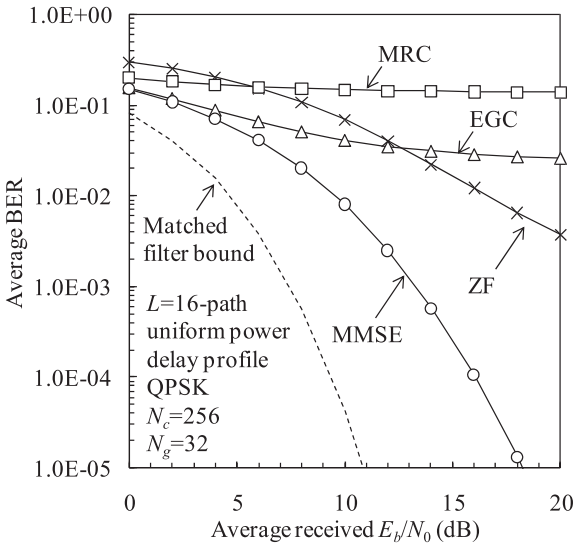

Fig. 3 BER performance of SC with FDE.

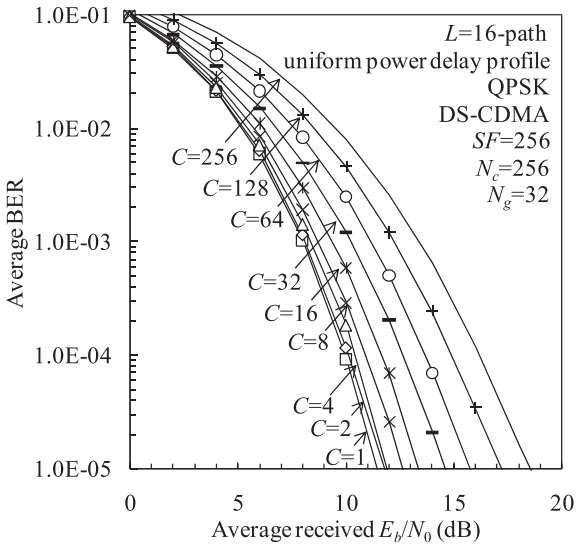

Fig. 4 BER performance of DS-CDMA with MMSE-FDE.

OFDM. $\hat{\boldsymbol{s}}$ is given as

$$\hat{\boldsymbol{s}} = \boldsymbol{F}^H \hat{\boldsymbol{R}} = \sqrt{\frac{2E_s}{T_s}} A\boldsymbol{s} + \boldsymbol{F}^H \boldsymbol{M} + \boldsymbol{F}^H \boldsymbol{W}\boldsymbol{N}. \tag{20}$$

The 1st term is a scaled version of the transmitted signal vector $\boldsymbol{s}$ and the 2nd and 3rd terms are respectively the residual ISI and noise after equalization.

Using the ZF weight (i.e., $\boldsymbol{W} = \boldsymbol{H}^{-1}$), the frequency-nonselective channel can be perfectly restored since $\hat{\boldsymbol{H}} = \boldsymbol{I}$ and $A = 1$ and as a consequence, the residual ISI disappears (i.e., $\boldsymbol{M} = \boldsymbol{0}$) in Eq. (20) (of course, this is the case if the channel estimation is ideal), but the noise after equalization is enhanced at a frequency where the channel gain drops. The MRC weight (i.e., $\boldsymbol{W} = \boldsymbol{H}^H$) enhances the frequency selectivity of the equivalent channel seen after equalization. The EGC weight only compensates for the phase rotation introduced by the channel selectivity. The MMSE weight minimizes the mean square of the equalization error defined as $e(k) = W(k)R(k) - S(k)$. In MMSE-FDE, since $\boldsymbol{W} \approx \boldsymbol{H}^{-1}$ except for the frequency where $|H(k)| \approx 0$, a near frequency-nonselective channel can be restored while alleviating the noise enhancement problem.

Figure 3 illustrates the achievable BER performance of SC with FDE. The channel is assumed to be a frequency-selective block Rayleigh fading channel having an $L = 16$-path uniform power delay profile ($E[|h_l|^2] = 1/L$). Among the four FDE weights, the MMSE weight can provide the best compromise between the noise enhancement and the suppression of frequency-selectivity and therefore, gives the best BER performance.

FDE can also be applied to orthogonal multicode DS-CDMA [12], [13]. FDE is a key technique for both MC- and DS-CDMA. So far, many studies have been done to improve the transmission performance of MC- and DS-CDMA with FDE. The MMSE-FDE also provides the best BER performance. The MMSE weight is given as

$$W(k) = \frac{H^*(k)}{|H(k)|^2 + (C/SF)^{-1}(E_s/N_0)^{-1}}, \tag{21}$$

where SF and C represent the spreading factor and the code multiplexing order, respectively.

Figure 4 illustrates the achievable average BER performance of DS-CDMA with MMSE-FDE. As the equivalent spreading factor, SF_{eq} ($= SF/C$), increases, the residual ICI can be further suppressed and the BER performance improves.

Another interesting application area for SC with FDE is optical communication systems in the presence of AWGN [27], [28].

4.2 Channel Capacity of FDE

The channel capacity analysis of SC transmission is an interesting study topic. In [29], the achievable channel capacity of SC transmission with FDE in a frequency-selective channel is theoretically examined and compared to that of OFDM. Below, the channel capacities of OFDM and SC with FDE are compared.

The estimate $\hat{\boldsymbol{s}} = [\hat{s}(0), \ldots, \hat{s}(t), \ldots, \hat{s}(N_c - 1)]^T$ of the transmitted symbol vector $\boldsymbol{s}$ is given by Eq. (20). The sum of the residual ISI and the noise is treated as a new white Gaussian noise. The signal-to-noise power ratio (SNR) is identical for all symbols in a block and the conditional SNR for the given $\boldsymbol{H}$ is given by

$$\begin{aligned}\gamma_{SC} &= \frac{\frac{2E_s}{T_s}|A|^2 \,\mathrm{tr}\{E[\boldsymbol{s}\boldsymbol{s}^H]\}}{\mathrm{tr}\{E[(\boldsymbol{F}^H\boldsymbol{M})(\boldsymbol{F}^H\boldsymbol{M})^H]\} + \mathrm{tr}\{E[(\boldsymbol{F}^H\boldsymbol{W}\boldsymbol{N})(\boldsymbol{F}^H\boldsymbol{W}\boldsymbol{N})^H]\}} \\ &= \frac{\frac{E_s}{N_0}|A|^2}{\frac{E_s}{N_0}\sum_{k=0}^{N_c-1}\left|\hat{H}(k) - A\right|^2 + \sum_{k=0}^{N_c-1}|W(k)|^2},\end{aligned} \tag{22}$$

where tr{$\boldsymbol{U}$} is the trace of the matrix $\boldsymbol{U}$. In the case of ZF-FDE, since $\boldsymbol{W} = \boldsymbol{H}^{-1}$ and $\hat{H}(k) = A = 1$, we have

$$\gamma_{SC-ZF} = \frac{E_s}{N_0} \cdot \frac{N_c}{\mathrm{tr}\{(\boldsymbol{H}^{-1})^H \boldsymbol{H}^{-1}\}} = \left(\frac{1}{N_c} \sum_{k=0}^{N_c-1} \frac{1}{\gamma(k)} \right)^{-1}, \quad (23)$$

where

$$\gamma(k) = \frac{E_s}{N_0} |H(k)|^2. \quad (24)$$

The conditional channel capacity (bps/Hz) of SC with ZF-FDE is given as

$$\begin{aligned} C_{SC-ZF} &= \log_2 (1 + \gamma_{SC-ZF}) \\ &= \log_2 \left[1 + \frac{E_s}{N_0} \left(\frac{1}{N_c} \sum_{k=0}^{N_c-1} |H(k)|^{-2} \right)^{-1} \right]. \end{aligned} \quad (25)$$

Unfortunately, closed form expressions for the conditional channel capacities achievable by the use of MMSE- and MRC-FDE are not found.

In the case of OFDM, the frequency-domain received signal vector, $\boldsymbol{R}$, can be written as

$$\boldsymbol{R} = \sqrt{\frac{2E_s}{T_s}} \boldsymbol{H}\boldsymbol{s} + \boldsymbol{N}. \quad (26)$$

The SNR is different for a different subcarrier. The SNR of the k-th subcarrier is given by $\gamma(k)$ and the conditional channel capacity of OFDM is given as

$$\begin{aligned} C_{OFDM} &= \frac{1}{N_c} \sum_{k=0}^{N_c-1} \log_2 (1 + \gamma(k)) \\ &= \frac{1}{N_c} \sum_{k=0}^{N_c-1} \log_2 \left(1 + \frac{E_s}{N_0} |H(k)|^2 \right). \end{aligned} \quad (27)$$

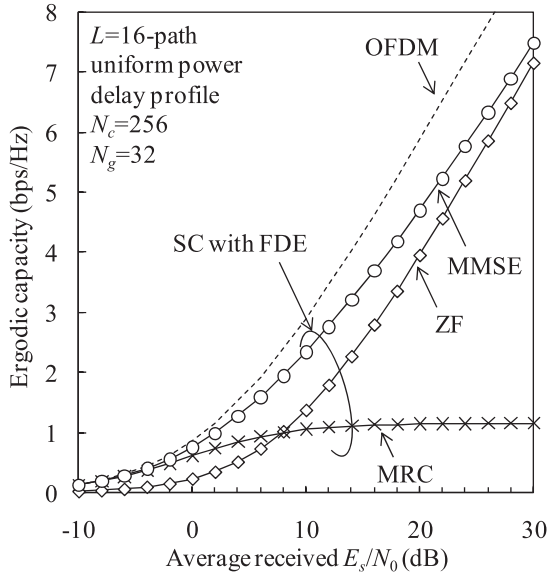

Fig. 5 Capacity comparison between SC with FDE and OFDM.

It can be shown from Jensen's inequality [30] that $C_{OFDM} \geq C_{SC-ZF}$ always (this is also confirmed in [31]). The conditional channel capacity for MRC- and MMSE-FDE can be computed using Eq. (22). The ergodic capacity is obtained by averaging the conditional channel capacity over all possible realizations of $\boldsymbol{H}$. Figure 5 compares the ergodic capacities of SC with ZF-, MRC-, and MMSE-FDE and OFDM. MMSE-, MRC-, and ZF-FDE provide lower capacity than OFDM. This is due to the presence of residual ISI for MMSE- and MRC-FDE and is due to the noise enhancement for ZF-FDE. However, it should be noted that for a low E_s/N_0 region, MMSE- and MRC-FDE provide almost identical channel capacity to OFDM.

5. Advanced FDE

First, the principle of overlap FDE that can improve the transmission efficiency by avoiding the GI insertion is presented. Then, a fractionally spaced FDE that can achieve the frequency diversity gain is described.

5.1 Overlap FDE

As explained in Sect. 4.1, in SC with FDE, the GI is added in front of each block to avoid the IBI from the previous block and a CP is inserted into the GI to make the received signal block a circular convolution of the transmitted N_c-symbol block and the channel impulse response. Because of this, the received signal block can be transformed by using the N_c-point FFT into the frequency-domain signal without distortion. However, the transmission efficiency is reduced by the insertion of the GI. If the GI insertion is not used, the IBI is present at the beginning of the received N_c-symbol block (see Fig. 6).

The reception of one symbol block during the time interval of $t = 0 \sim (N_c - 1)$ is considered. The received signal is given as Eq. (3). The desired signal component must be expressed as a circular convolution of the transmitted N_c-symbol block and the channel impulse response to obtain the frequency-domain received signal as Eq. (7). With the CP insertion into the GI, the received signal is given as Eq. (4). On the other hand, without GI insertion, the IBI appears. In such a case, the received signal can be expressed as

$$r(t) = \sqrt{\frac{2E_s}{T_s}} \sum_{l=0}^{L-1} h_l s((t-\tau_l) \bmod N_c) + \nu(t) + n(t), \quad (28)$$

where $\nu(t)$ represents the IBI component given as

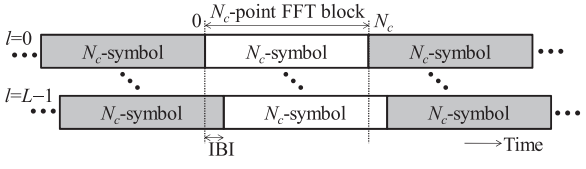

Fig. 6 FFT interval and IBI.

$$v(t) = \sqrt{\frac{2E_s}{T_s}} \sum_{l=0}^{L-1} h_l \{s(t-\tau_l) - s((t-\tau_l) \bmod N_c)\} \times \{u(t) - u(t-\tau_l)\} \quad (29)$$

with $u(t) = 0$ (1) for $t < 0$ ($0 \le t$). The BER performance of SC with FDE without GI insertion degrades due to the presence of IBI.

Recently, overlap-save signal processing using FFT [32] was applied to SC with FDE in literature [33]–[36] (referred to as overlap FDE hereafter). The paper that first mentioned the application of overlap FDE to SC transmission is perhaps [33]. The principle of overlap FDE is given below.

MMSE-FDE is viewed as a circular linear filter. The impulse response $h_{MMSE-FDE}(\tau)$ of the MMSE-FDE circular filter concentrates only at the vicinity of $\tau = 0$ as seen in Fig. 7. This fact can be utilized to avoid the GI insertion. The IBI can be suppressed by overlapping the FFT block, and selecting only the middle M-symbol portion from the N_c-symbol block for data demodulation as shown in Fig. 8. Using a smaller M can reduce the residual IBI. The BER performance of the overlap FDE is plotted in Fig. 9 as a function of the average received E_b/N_0. By choosing a sufficiently small M, BER performance close to that for the conventional FDE can be achieved; however, the computational complexity increases since the number of FFT/IFFT operations per N_c-symbol block increases by N_c/M times.

The overlap FDE can also be applied to DS-CDMA to improve the transmission efficiency while achieving the frequency diversity gain. The application of FDE to a CDMA downlink can be found in [34]. Three FDE implementations are considered: CP insertion (into the GI), zero-padding, and overlap FDE. In the zero-padding method, N_g zeros are added to the end of an $(N_c - N_g)$-symbol block to build an N_c-symbol block before transmission. At the receiver, an N_c-point FFT is applied to the zero-padded data block and the detected zeros at the end of this data block are then discarded. Although both the CP and zero-padding methods divide the data stream into blocks of data by adding redundancy, the overlap FDE does not require any redundancy. The overlap FDE can approximate the performance of the other two methods very well.

The overlap FDE can be applied to the present DS-CDMA systems without modifying the air interface of 3G systems. Therefore, it is a very attractive equalization technique. How the packet throughput in a DS-CDMA system can be improved is discussed in [36]. The MMSE-FDE weight for packet combining in hybrid automatic repeat request (HARQ) is derived. The overlap FDE provides better throughput performance than both coherent rake combining and conventional FDE irrespective of the degree of channel frequency-selectivity. Figure 10 plots the achievable throughput performances of DS-CDMA using overlap FDE, conventional FDE, and coherent rake combining, as a function of the average received E_s/N_0 [37]. Full code-multiplexing using the spreading factor $SF = 16$ and the code-multiplexing order $C = 16$ is assumed (therefore, the transmission symbol rate is the same as the nonspread SC signal transmission). As an error control technique, an HARQ with incremental redundancy strategy (IR) using type II S-P2 [38] is used.

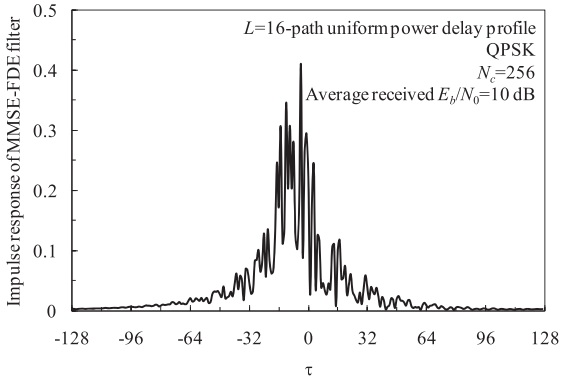

Fig. 7 Impulse response of MMSE-FDE circular filter.

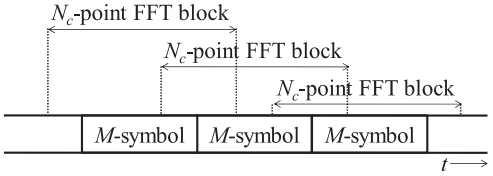

Fig. 8 Overlap FDE.

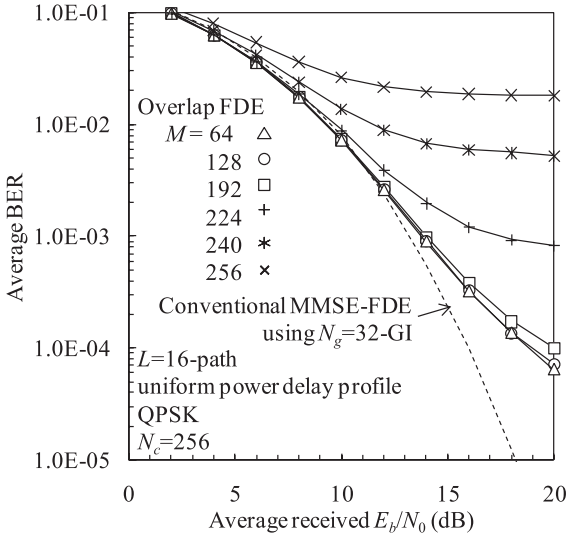

Fig. 9 BER performance of overlap FDE.

As discussed earlier, the residual ICI (or ISI in the case of the nonspread SC signal transmission) limits the performance improvement. Although the impulse response of the MMSE-FDE circular filter is concentrated in the immediate vicinity of $\tau = 0$ (see Fig. 7), it is still spread over a relatively wide range of time. This causes residual IBI even after application of the overlap FDE. The residual ICI and IBI can be suppressed by repeating joint MMSE-FDE and ICI cancellation a sufficient number of times and selecting the

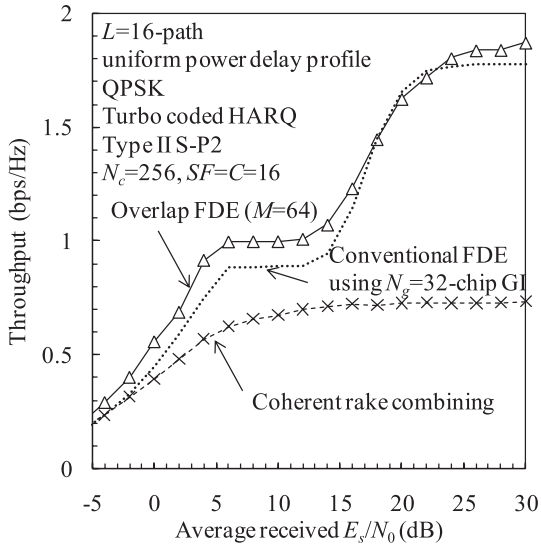

Fig. 10 Throughput performance of DS-CDMA with overlap FDE.

middle M-chip portion from the N_c-chip block [35]. If the ICI is sufficiently suppressed, the MMSE weight approaches the MRC weight. The impulse response of the MRC-FDE circular filter is given by $h_{MRC-FDE}(\tau) = h^*(-\tau)$. Therefore, the use of the MRC weight gives the matched filter bound (the IBI is spread only within the maximum time delay, τ_{max}, of the channel and hence the residual IBI can be perfectly removed).

5.2 Fractionally Spaced FDE (FSE)

Fractionally spaced FDE (called FSE in this paper) was proposed to offer further performance improvement of OFDM [39] and SC [40], [41]. OFDM with conventional FDE cannot obtain the frequency diversity gain since each data symbol is transmitted on a single subcarrier. However, the use of FSE can achieve the frequency diversity gain [39]. How the FSE can be applied to SC is presented in [40]. In [40], a zero-forcing FSE is considered and it is shown that a certain freedom exists in the choice of the equalizer coefficients. This freedom is then utilized to minimize the influence of additive noise at the detector input. The frequency diversity gain acquired through this approach depends on the signal spectral shape and its excess bandwidth.

In [41], a general case of G-oversampling FSE is considered, where G is a positive integer, and the optimum FDE weight is derived based on ZF and the MMSE criteria. Figure 11 illustrates the transmission system model of SC with G-oversampling FSE. Below, the G-oversampling FSE is described.

The transmit symbol block can be written as

$$s(t) = \sqrt{\frac{2E_s}{T_s}} \sum_{q=0}^{N_c-1} s_q \delta(t - qT_s), \tag{30}$$

where s_q is the q-th data symbol and T_s is the symbol duration. After inserting an N_g-symbol CP into the GI, the

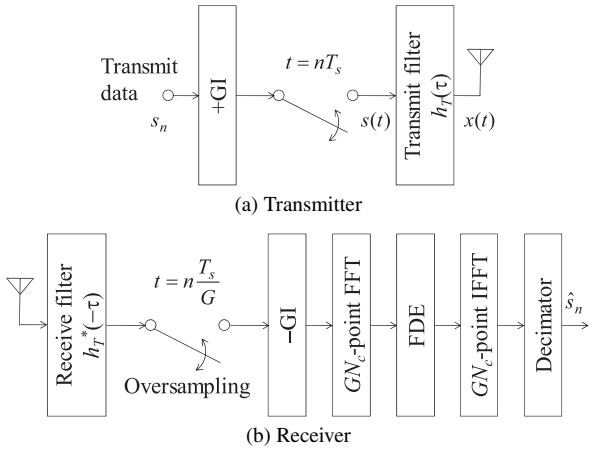

Fig. 11 Transmission system model of SC with FSE.

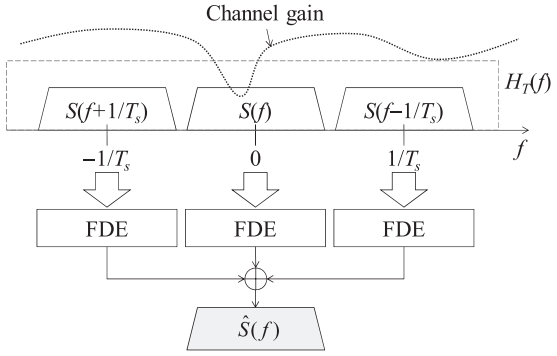

Fig. 12 Transmit spectrum and G-oversampling FSE for SC (G = 3).

transmit symbol block is input to the transmit filter with impulse response $h_T(\tau)$. The transmitted signal, $x(t)$, is written as

$$x(t) = \int s(t-\tau) h_T(\tau) d\tau. \tag{31}$$

The Fourier transform of $s(t)$ is a periodic function with period $1/T_s$ and can be expressed as $\sum_m S(f - m/T_s)$, where $S(f)$ is defined over $-1/(2T_s) \le f < 1/(2T_s)$. Fourier transform $X(f)$ of $x(t)$ is given by

$$\begin{aligned} X(f) &= \int_{-\infty}^{+\infty} x(t) \exp(-j2\pi f t) dt \\ &= \frac{1}{T_s} H_T(f) \sum_m S\left(f - \frac{m}{T_s}\right), \end{aligned} \tag{32}$$

where $H_T(f)$ is the Fourier transform of $h_T(\tau)$. As can be understood from Eq. (32), multiple copies of the signal spectrum are transmitted simultaneously. This can be utilized to achieve the additional frequency diversity gain at the receiver by oversampling the received signal as shown in Fig. 12.

At the receiver, matched filter $h_T^*(-\tau)$ is used. The received signal is sampled at rate G/T_s. The received signal sampled at $t = (q + g/G)T_s$, $q = 0 \sim (N_c - 1)$ and $g = 0 \sim (G - 1)$, is given by

$$r(t) = \int s(t-\tau)\tilde{h}(\tau)d\tau + n(t), \tag{33}$$

where $\tilde{h}(\tau)$ is the impulse response of the composite channel (transmit filter + propagation channel + receive filter). Assume that $\tilde{h}(\tau)$ is limited within the GI. Since $s(x) = 0$ if x is not an integer, Eq. (33) can be expressed using the matrix form as

$$\begin{aligned} \boldsymbol{r}' &= \left[r(0), r\left(\frac{1}{G}\right), \cdots, r\left(q+\frac{g}{G}\right), \cdots, r\left(N_c - \frac{1}{G}\right)\right]^T \\ &= \boldsymbol{h}'\boldsymbol{U}\boldsymbol{s} + \boldsymbol{n}', \end{aligned} \tag{34}$$

where $\boldsymbol{h}'$ is a $GN_c \times GN_c$ circulant matrix of the composite channel impulse response, $\boldsymbol{s} = [s_0, \ldots, s_q, \ldots, s_{Nc-1}]^T$ is the transmitted symbol vector, and $\boldsymbol{n}' = [n(0), n(1/G), \ldots, n(q+g/G), \ldots, n(N_c - 1/G)]^T$ is the noise vector. $\boldsymbol{U}$ is called the expander matrix of size $GN_c \times N_c$, whose $G \times k$-th row is the k-th row of the $N_c \times N_c$ identity matrix $\boldsymbol{I}$ and the other rows are zero. Similar to $\boldsymbol{h}$ in Eq. (5), the circulant matrix $\boldsymbol{h}'$ can be expressed as $\boldsymbol{h}' = \boldsymbol{F}_G^H \boldsymbol{H}' \boldsymbol{F}_G$, where $\boldsymbol{F}_G$ is a $GN_c \times GN_c$ FFT matrix and $\boldsymbol{H}' = \mathrm{diag}\{H(0), \ldots, H(k), \ldots, H(GN_c - 1)\}$. Therefore, Eq. (34) can be rewritten as

$$\boldsymbol{r}' = \boldsymbol{A}\boldsymbol{s} + \boldsymbol{n}'. \tag{35}$$

with $\boldsymbol{A} = \boldsymbol{F}_G^H \boldsymbol{H}' \boldsymbol{F}_G \boldsymbol{U}$. In Ref. [39], the FSE multiplies $\boldsymbol{r}'$ by $\boldsymbol{A}^H$ and replaces $\boldsymbol{H}'$ with $\boldsymbol{W}'$. The FSE output vector, $\hat{\boldsymbol{s}}$, is the estimate of the transmitted symbol vector $\boldsymbol{s}$ and is given by

$$\hat{\boldsymbol{s}} = \left(\boldsymbol{U}^H \boldsymbol{F}_G^H \boldsymbol{W}' \boldsymbol{F}_G\right)\boldsymbol{r}', \tag{36}$$

where $\boldsymbol{W}' = \mathrm{diag}\{W(0), \ldots, W(k), \ldots, W(GN_c - 1)\}$ is the FDE weight matrix. Since

$$\boldsymbol{F}_G \boldsymbol{U} = \frac{1}{\sqrt{G}} \begin{bmatrix} \boldsymbol{I} \\ \vdots \\ \boldsymbol{I} \end{bmatrix} \boldsymbol{F}, \tag{37}$$

Eq. (36) can be rewritten as

$$\begin{aligned} \hat{\boldsymbol{s}} = {} & \frac{1}{G}\boldsymbol{F}^H \left[\boldsymbol{W}'_0 \boldsymbol{H}'_0 + \cdots + \boldsymbol{W}'_g \boldsymbol{H}'_g + \cdots + \boldsymbol{W}'_{G-1} \boldsymbol{H}'_{G-1}\right] \\ & \cdot \boldsymbol{F}_G \boldsymbol{s} + \frac{1}{\sqrt{G}} \boldsymbol{F}^H \left[\boldsymbol{W}'_0, \cdots, \boldsymbol{W}'_g, \cdots, \boldsymbol{W}'_{G-1}\right] \boldsymbol{F}_G \boldsymbol{n}', \end{aligned} \tag{38}$$

where $\boldsymbol{H}'_g = \mathrm{diag}\{H(gN_c), \ldots, H((g+1)N_c - 1)\}$ and $\boldsymbol{W}'_g = \mathrm{diag}\{W(gN_c), \ldots, W((g+1)N_c - 1)\}$ for $g = 0 \sim G - 1$.

Equation (38) shows that the received multiple copies of the original signal spectrum are added together. The spectrum distortion due to the channel frequency selectivity can be suppressed by adding the multiple copies of the spectrum, thereby achieving a higher frequency diversity gain.

6. Residual Inter-Symbol Interference (ISI) Cancellation

Although one-tap MMSE-FDE can significantly improve the BER performance of SC signal transmission, a big performance gap still exists from the theoretical lower bound. This is due to the presence of residual ISI after MMSE-FDE. A residual ISI cancellation technique can be introduced into MMSE-FDE to improve the BER performance. The receiver structure of joint MMSE-FDE and residual ISI cancellation is illustrated in Fig. 13.

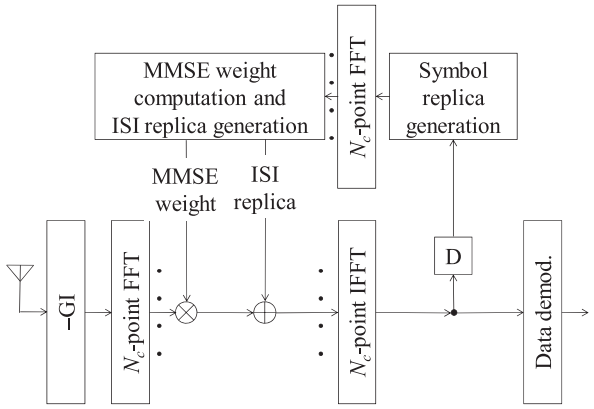

Fig. 13 MMSE-FDE and residual ISI cancellation. Uncoded transmission case.

The frequency-domain received signal, $\hat{\boldsymbol{R}}$, after FDE is given by Eq. (13). The replica of the residual ISI vector $\boldsymbol{M}$ is generated and subtracted from $\hat{\boldsymbol{R}}$. MMSE-FDE and residual ISI cancellation can be repeated in an iterative fashion so as to improve the accuracy of the ISI replica generation. The i-th iteration is described below.

After performing MMSE-FDE using weight matrix $\boldsymbol{W}^{(i)} = \mathrm{diag}\{W^{(i)}(0), \cdots, W^{(i)}(k), \cdots, W^{(i)}(N_c - 1)\}$, residual ISI cancellation is performed in the frequency-domain as

$$\tilde{\boldsymbol{R}}^{(i)} = \hat{\boldsymbol{R}}^{(i)} - \tilde{\boldsymbol{M}}^{(i)}, \tag{39}$$

where $\tilde{\boldsymbol{M}}^{(i)}$ is generated as

$$\tilde{\boldsymbol{M}}^{(i)} = \sqrt{\frac{2E_s}{T_s}} \left\{\hat{\boldsymbol{H}}^{(i)} - A^{(i)}\boldsymbol{I}\right\} \boldsymbol{F}\tilde{\boldsymbol{s}}^{(i-1)} \tag{40}$$

with $\hat{\boldsymbol{H}}^{(i)} = \boldsymbol{W}^{(i)}\boldsymbol{H}$ and $\tilde{\boldsymbol{s}}^{(-1)} = \boldsymbol{0}$, where $\tilde{\boldsymbol{s}}^{(i-1)}$ represents the soft replica of the transmitted symbol block (which is generated by feeding back the log likelihood ratios (LLRs) obtained at the $(i-1)$-th stage). Then, the N_c-point IFFT is performed on $\tilde{\boldsymbol{R}}^{(i)}$ to obtain the estimate of the transmitted symbol vector.

A series comprising joint MMSE-FDE and residual ISI cancellation, N_c-point IFFT, and data replica generation is repeated a sufficient number of times. Finally, data-demodulation is carried out to recover the transmitted data.

The equalization error vector, $\boldsymbol{e}^{(i)}$, between $\tilde{\boldsymbol{R}}^{(i)}$ and $\boldsymbol{S}(= \boldsymbol{F}\boldsymbol{s})$ is defined as

$$\begin{aligned} \boldsymbol{e}^{(i)} &= \tilde{\boldsymbol{R}}^{(i)} - A^{(i)}\boldsymbol{F}\boldsymbol{s} \\ &= \sqrt{\frac{2E_s}{T_s}} \left(\hat{\boldsymbol{H}}^{(i)} - A^{(i)}\boldsymbol{I}\right) \boldsymbol{F}\left(\boldsymbol{s} - \tilde{\boldsymbol{s}}^{(i-1)}\right) + \boldsymbol{W}^{(i)}\boldsymbol{N}. \end{aligned} \tag{41}$$

Since N_c data symbols in a block are independent and identically distributed, the covariance matrix, $E[\boldsymbol{e}^{(i)}\{\boldsymbol{e}^{(i)}\}^H]$, of $\boldsymbol{e}^{(i)}$

is diagonal and its k-th diagonal element is given by

$$E[|e^{(i)}(k)|^2] = \frac{2E_s}{T_s}\left|\hat{H}^{(i)}(k) - A^{(i)}\right|^2 \cdot \rho^{(i-1)} + \frac{2N_0}{T_s}\sum_{k'=0}^{N_c-1}\left|W^{(i)}(k')\right|^2, \quad (42)$$

where $\rho^{(i-1)} = E[|s(t) - \tilde{s}^{(i-1)}(t)|^2]$. The MMSE weight vector $\boldsymbol{W}^{(i)}$ minimizes the MSE $E[|e^{(i)}(k)|^2]$, $k = 0 \sim (N_c - 1)$, for the given $\boldsymbol{H}$. By solving $\partial E[|e^{(i)}(k)|^2]/\partial W^{(i)}(k) = 0$, the MMSE weight $W^{(i)}(k)$ is derived as [42]

$$W^{(i)}(k) = \frac{H^*(k)}{\rho^{(i-1)}|H(k)|^2 + (E_s/N_0)^{-1}}. \quad (43)$$

For QPSK data modulation ($s(t) = (a(t) + jb(t))/\sqrt{2}$ with $a(t)$ and $b(t) = \pm 1$), the soft replica of the t-th symbol, $\tilde{s}^{(i-1)}(t)$, can be generated using the *a posteriori* probabilities of $a(t)$ and $b(t)$ as

$$\tilde{s}^{(i-1)}(t) = \frac{1}{\sqrt{2}}\left(a(t)\tanh\frac{a(t)\lambda_a(t)}{2} + jb(t)\tanh\frac{b(t)\lambda_b(t)}{2}\right), \quad (44)$$

where $\lambda_a(t)$ and $\lambda_b(t)$ are the LLRs of $a(t)$ and $b(t)$, respectively, and $\tanh x = (e^x - e^{-x})/(e^x + e^{-x})$. Therefore, we have

$$\rho^{(i-1)} = E[|s(t) - \tilde{s}^{(i-1)}(t)|^2 = E\left[2\left(e^{a(t)\lambda_a^{(i-1)}(t)} + 1\right)^{-2} + 2\left(e^{b(t)\lambda_b^{(i-1)}(t)} + 1\right)^{-2}\right]. \quad (45)$$

However, $a(t)$ and $b(t)$ are unknown to the receiver. We replace the ensemble average of Eq. (45) by the average using the *a posteriori* probabilities of $a(t)$ and $b(t)$ and further replace it by the block average over an N_c-symbol block. We obtain [43]

$$\rho^{(i-1)} = \frac{2}{N_c}\sum_{t=0}^{N_c-1}\left[\frac{e^{\lambda_a^{(i-1)}(t)}}{\left(e^{\lambda_a^{(i-1)}(t)} + 1\right)^2} + \frac{e^{\lambda_b^{(i-1)}(t)}}{\left(e^{\lambda_b^{(i-1)}(t)} + 1\right)^2}\right]. \quad (46)$$

As i increases, the residual ISI gradually reduces and consequently, $\rho^{(i-1)}$ reduces. As a consequence, the MMSE weight $W^{(i)}(k)$ approaches the MRC weight.

Figure 14 shows the BER performance of MMSE-FDE using frequency-domain ISI cancellation. It can be seen from the figure that the residual ISI cancellation significantly improves the BER performance of SC with FDE and reduces the performance gap from the matched filter bound. The idea of residual ISI cancellation can also be applied to DS-CDMA with FDE in order to significantly improve its BER performance [42].

In the above, an uncoded transmission is assumed and equalization/residual ISI cancellation is done in an iterative fashion within each received signal block. However, in a coded transmission system, the above described iterative equalization/residual ISI cancellation and channel decoding can be jointly performed using the turbo equalization principle [26].

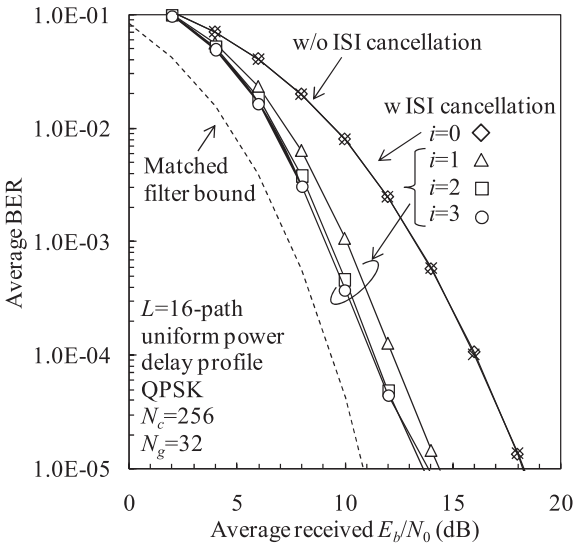

Fig. 14 BER performance of SC with MMSE-FDE and residual ISI cancellation.

7. Channel Estimation (CE)

Accurate estimation of channel gain $H(k)$ and the received SNR are necessary for MMSE-FDE. Many studies on channel estimation (CE) can be found for OFDM signal transmission. Frequency-domain CE techniques based on the MMSE and least square (LS) criteria were proposed in [44]. It is shown in [44] that MMSE-CE is superior to LS-CE with respect to the estimation accuracy, while LS-CE has a lower complexity level.

The channel impulse response is assumed to be limited within the GI length. This can be utilized by the delay time-domain windowing technique to improve the channel estimation accuracy [44].

A pilot-assisted CE with a single 2D (joint time- and frequency-domains) filter and that with two separated 1D (independent time- and frequency-domains) filters based on the MMSE criterion can also be used. The performance of the joint 2D filter is similar to that for two 1D filters and outperforms the performance of a single 1D filter with respect to overhead, MSE, and latency [45].

Pilot-assisted CE developed for OFDM cannot be directly applied to SC with FDE. This is because, if a pseudo noise (PN) sequence is used as the pilot, its amplitude of the pilot block varies in the frequency-domain over the signal bandwidth and the noise enhancement problem is produced. Of course, the Chu sequence [46], which has a constant amplitude in both the time- and frequency-domains, can be used as the pilot; however, the number of Chu sequences is limited. Therefore, the use of PN sequence may be still of practical importance since a large number of pilot sequences can be generated.

Frequency-domain channel estimation methods for SC with FDE can be found in [47]. Two different approaches were proposed that use pilot blocks transmitted prior to a

sequence of data blocks: the first operates independently on each frequency while the second utilizes the fading correlation across the signal bandwidth. The least mean square (LMS) and recursive least square (RLS) algorithms are employed to update the channel estimates.

In order to make the channel estimation accuracy almost insensitive to the choice of the PN pilot sequence, the MMSE-CE was proposed for SC with FDE in [48] and [49]. The k-th frequency component of the received pilot block can be expressed as

$$R(k) = \sqrt{\frac{2E_s}{T_s}}H(k)P(k) + N(k), \tag{47}$$

where $P(k)$ and $N(k)$ are the k-th frequency component of the pilot block and the noise due to the AWGN, respectively. $\sqrt{2E_s/T_s}H(k)$ is unknown to the receiver. MMSE-CE is employed to obtain channel estimate $\breve{H}(k)$ as

$$\breve{H}(k) = X(k)R(k). \tag{48}$$

Since $P(k)$ is not constant, spectrum nulls in the pilot spectrum sometimes occur. For MMSE-CE, estimation error $e(k)$ between $\sqrt{2E_s/T_s}H(k)$ and $\breve{H}(k)$ is defined as

$$e(k) = \breve{H}(k) - \sqrt{2E_s/T_s}H(k). \tag{49}$$

The optimum $X(k)$ that minimizes the MSE $E[|e(k)|^2]$ for the given $P(k)$ can be derived by solving $\partial E[|e(k)|^2]/\partial X(k) = 0$ (under the condition $E\left[|H(k)|^2\right] = 1$) as

$$X(k) = \frac{P^*(k)}{|P(k)|^2 + (E_s/N_0)^{-1}}. \tag{50}$$

The MMSE channel estimator for SC with FDE in an ultra-wideband (UWB) channel is derived in [48], which provides only a small degree of performance degradation compared to the perfect channel estimation case. An extension of the frequency-domain MMSE channel estimation to DS-CDMA with FDE is shown in [49]. Even if MMSE-CE is used, the channel estimate is perturbed by the noise due to the AWGN. The delay time-domain windowing technique can be used to reduce the noise. A higher tracking ability against time-varying channel can be achieved by decision feedback of the previous block decision results.

Figure 15 shows the structure of MMSE-CE using the delay time-domain windowing and decision feedback. The actual channel impulse response is limited within the GI length while the noise due to the AWGN is uniformly distributed over the entire delay time range. Therefore, the noise can be suppressed by replacing the estimated channel impulse response with zeros (or zero-padding) beyond the GI. After applying the N_c-point FFT, the improved channel gain estimate, $\tilde{H}(k)$, is obtained as

$$\tilde{H}(k) = \sum_{k'=0}^{N_c-1} \breve{H}(k')\omega(k-k'), \tag{51}$$

where

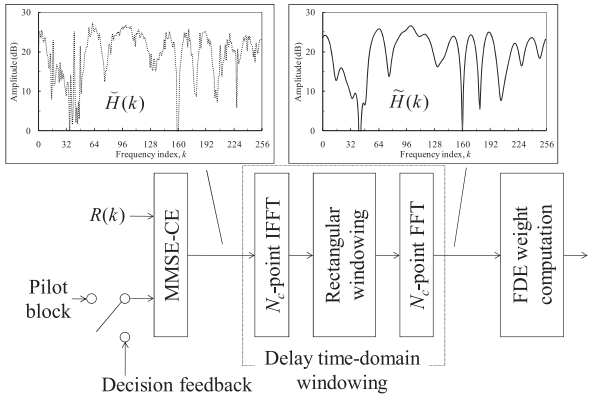

Fig. 15 MMSE-CE with delay time-domain windowing and decision feedback.

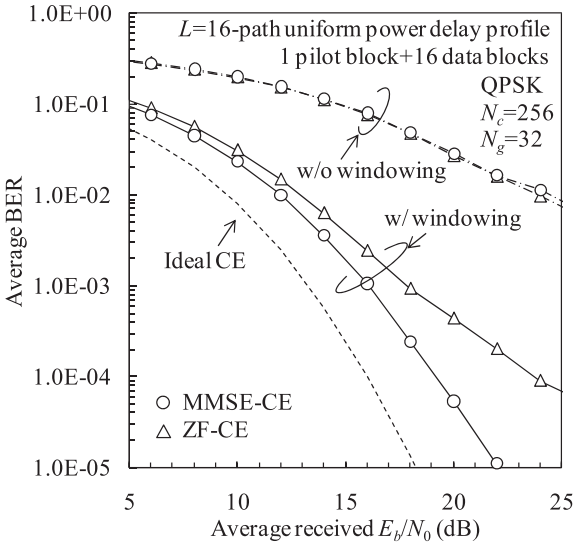

Fig. 16 BER performance of MMSE-CE.

$$\omega(x) = \frac{1}{N_c}\frac{\sin\left(\pi\frac{N_g}{N_c}x\right)}{\sin\left(\pi\frac{1}{N_c}x\right)}\exp\left(j\pi\frac{N_g-1}{N_c}x\right). \tag{52}$$

However, when decision feedback is used, decision error propagates. To eliminate the error propagation, low-pass filtering can be applied to past channel estimates.

The BER performances of SC with FDE using pilot-assisted ZF-CE, i.e., $X(k) = 1/P(k)$, and MMSE-CE with delay time-domain windowing are plotted in Fig. 16. One pilot block is followed by 16 QPSK data blocks. A PN sequence is used for the pilot. The BER performance of ZF-CE degrades due to the existence of the pilot spectrum nulls. On the other hand, MMSE-CE is not sensitive to the pilot spectrum shape and hence, provides better BER performance. The BER performance without delay time-domain windowing is plotted for comparison in Fig. 16. The figure shows that the delay time-domain windowing technique reduces the noise and significantly improves the BER performance.

The GI insertion can be utilized to achieve good channel estimation in a fast-fading environment since it is contained in every block. A known short pilot sequence whose length is equal to the GI is appended as a suffix to every data block before inserting a CP into the GI. Since the suffix of the previous block acts as the CP of the present block, channel estimation can be done by using the N_g-point FFT (where N_g is the GI length) and frequency-domain interpolation [50]. Also, joint data detection and channel estimation can be performed after the N_c-point FFT [51]. The data block imparts severe interference to the channel estimate and iterative channel estimation becomes necessary; however, only the use of two iterations is sufficient.

8. MIMO Applications for SC with FDE

MIMO antenna techniques can be used to achieve improved transmission performance and higher throughput without bandwidth expansion [52]. MIMO techniques can be roughly classified into three categories: antenna diversity, adaptive antenna array (AAA), space division multiplexing (SDM). FDE can be jointly used with the above MIMO techniques to improve further the SC transmission performance in a strong frequency-selective channel.

8.1 Antenna Diversity

8.1.1 Receive Antenna Diversity

The antenna diversity technique can increase the received SNR and hence improve the transmission performance. There are two types of antenna diversity: receive antenna diversity and transmit antenna diversity. Receive antenna diversity has been successfully used in practical systems. The joint use of FDE and antenna diversity for SC signal transmission has been studied in [53] and [54].

Figure 17 shows the receiver structure of joint FDE and N_r-antenna diversity combining. After the removal of the GI, the N_c-point FFT is applied to transform the received signal block, $\{r_m(t);\ t = 0 \sim (N_c - 1)\}$, of the m-th receive antenna into the frequency-domain signal $\{R_m(k);\ k = 0 \sim (N_c - 1)\}$, $m = 0 \sim (N_r - 1)$. Joint FDE and antenna diversity combining can be done as

$$\hat{R}(k) = \sum_{m=0}^{N_r-1} W_m(k) R_m(k), \tag{53}$$

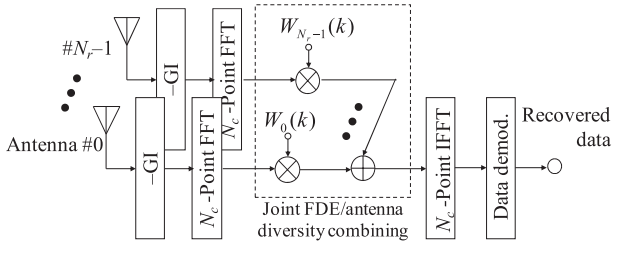

Fig. 17 Receiver structure of joint FDE/antenna diversity combining.

where $W_m(k)$ is the joint FDE/diversity combining weight based on the MMSE criterion and is given by [54]

$$W_m(k) = \frac{H_m^*(k)}{\sum_{m'=0}^{N_r-1} |H_{m'}(k)|^2 + (E_s/N_0)^{-1}}, \tag{54}$$

where $H_m(k)$ is the channel gain associated with the m-th receive antenna.

Figure 18 plots the achievable average BER performance. Both frequency diversity gain and space diversity gain can be achieved. As N_r increases, the BER performance consistently improves.

8.1.2 Transmit Antenna Diversity

Transmit antenna diversity is attractive for downlink applications since it can alleviate the complexity problem of mobile receivers. The well-known type of transmit antenna diversity is space-time block coded transmit diversity (STTD) [55] to achieve the space diversity gain. Cyclic delay transmit diversity (CDTD) is another well-known transmit diversity technique to achieve a large frequency diversity gain even in a weak frequency-selective channel [56], [57]. Both STTD and CDTD do not require channel state information (CSI) on the transmitter side.

To perform joint FDE/STTD decoding at the receiver, multiple consecutive signal blocks are encoded in the frequency-domain at the transmitter [53], [58], [59]. For N_t = 2-antenna frequency-domain STTD encoding, two consecutive (even and odd) signal blocks, $\{s_e(t);\ t = 0 \sim (N_c-1)\}$ and $\{s_o(t);\ t = 0 \sim (N_c - 1)\}$, are transformed using the N_c-point FFT into two (even and odd) frequency-domain signals, $\{S_e(k);\ k = 0 \sim (N_c - 1)\}$ and $\{S_o(k);\ k = 0 \sim (N_c - 1)\}$, respectively. N_t = 2-antenna frequency-domain STTD encoding is given in Table 1. After frequency-domain STTD

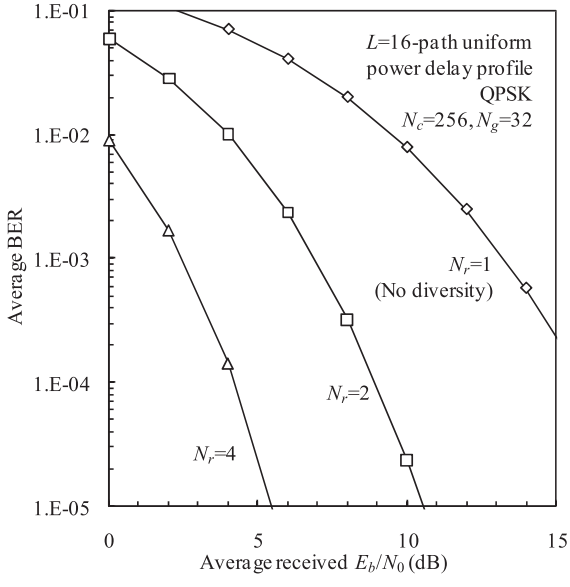

Fig. 18 BER performance of joint FDE/antenna diversity combining.

Table 1 Frequency-domain STTD encoding.

Time (in blocks)	Antenna #0	Antenna #1
Even	$\frac{1}{\sqrt{2}} S_e(k)$	$\frac{1}{\sqrt{2}} S_o(k)$
Odd	$-\frac{1}{\sqrt{2}} S_o^*(k)$	$\frac{1}{\sqrt{2}} S_e^*(k)$

Table 2 Equivalent time-domain STTD encoding.

Time (in blocks)	Antenna #0	Antenna #1
Even	$\frac{1}{\sqrt{2}} s_e(t)$	$\frac{1}{\sqrt{2}} s_o(t)$
Odd	$-\frac{1}{\sqrt{2}} s_o^*\big((N_c - t) \bmod N_c\big)$	$\frac{1}{\sqrt{2}} s_e^*\big((N_c - t) \bmod N_c\big)$

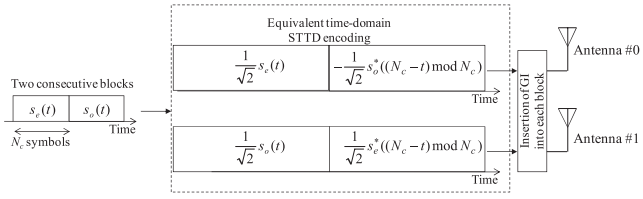

Fig. 19 Equivalent time-domain STTD encoding.

encoding, the N_c-point IFFT is used to obtain the time-domain STTD encoded signal blocks. The transmit power from each antenna is halved to keep the total transmit power the same.

The above frequency-domain encoding requires N_c-point FFT and IFFT operations. An equivalent time-domain STTD encoding that requires no FFT and IFFT operations can be derived using

$$\begin{cases} \dfrac{1}{N_c} \displaystyle\sum_{k=0}^{N_c-1} S_e^*(k) \exp\left(j2\pi t \frac{k}{N_c}\right) = s_e^*((N_c - t) \bmod N_c) \\ \dfrac{1}{N_c} \displaystyle\sum_{k=0}^{N_c-1} S_o^*(k) \exp\left(j2\pi t \frac{k}{N_c}\right) = s_o^*((N_c - t) \bmod N_c) \end{cases}. \quad (55)$$

The equivalent time-domain STTD encoding is given in Table 2 and is illustrated in Fig. 19.

At the receiver, after the removal of the GI, the even and odd signal blocks received at the m-th receive antenna are transformed using the N_c-point FFT into two (even and odd) frequency-domain signals, $\{R_{e,m}(k);\ k = 0 \sim (N_c - 1)\}$ and $\{R_{o,m}(k);\ k = 0 \sim (N_c - 1)\}$, $m = 0 \sim (N_r - 1)$. N_t = 2-antenna STTD decoding is carried out jointly with FDE and antenna diversity combining as

$$\begin{cases} \hat{R}_e(k) = \displaystyle\sum_{m=0}^{N_r-1} \left\{ W_{m,0}^*(k) R_{e,m}(k) + W_{m,1}(k) R_{o,m}^*(k) \right\} \\ \hat{R}_o(k) = \displaystyle\sum_{m=0}^{N_r-1} \left\{ W_{m,1}^*(k) R_{e,m}(k) - W_{m,0}(k) R_{o,m}^*(k) \right\} \end{cases}, \quad (56)$$

where $W_{m,n}(k)$, $n = 0$ or 1, is the MMSE weight given by

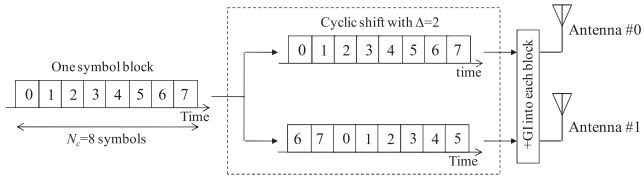

Fig. 20 Transmitter structure of CDTD for the case of $N_c = 8$ symbols.

$$W_{m,n}(k) = \frac{H_{m,n}(k)}{\dfrac{1}{2} \displaystyle\sum_{m'=0}^{N_r-1} \sum_{n'=0}^{1} |H_{m',n'}(k)|^2 + (E_s/N_0)^{-1}} \quad (57)$$

with $H_{m,n}(k)$ being the channel gain between the n-th transmit antenna and the m-th receive antenna. $H_{m,n}(k)$ is given as

$$H_{m,n}(k) = \sum_{l=0}^{L-1} h_{m,n,l} \exp\left(-j2\pi k \frac{\tau_l}{N_c}\right), \quad (58)$$

where $h_{m,n,l}$ represents the l-th path gain.

Finally, the N_c-point IFFT is applied to $\{\hat{R}_e(k)\}$ and $\{\hat{R}_o(k)\}$ to obtain the time-domain signal blocks for data demodulation.

For CDTD [60], [61], the same signal block is simultaneously transmitted from different transmit antennas after adding different cyclic delays as shown in Fig. 20. The transmitted signal block from the n-th transmit antenna ($n = 0 \sim (N_t - 1)$) is given by

$$s_n(t) = \sqrt{\frac{2E_s}{N_t T_s}} s((t - n\Delta) \bmod N_c), \quad (59)$$

where $n\Delta$ is the cyclic delay. At the receiver, the N_c-point FFT is applied to the signal block received at the m-th antenna to transform it into the frequency-domain signal, $\{R_m(k);\ k = 0 \sim (N_c - 1)\}$. One-tap FDE is carried out as

$$\hat{S}(k) = \sum_{m=0}^{N_r-1} W_{m,CDTD}(k) R_m(k), \quad (60)$$

where $W_{m,CDTD}(k)$ is the MMSE-FDE weight given by [60].

$$W_{m,CDTD}(k) = \frac{H_{m,CDTD}^*(k)}{\displaystyle\sum_{m'=0}^{N_r-1} |H_{m',CDTD}(k)|^2 + (E_s/N_0)^{-1}}. \quad (61)$$

In Eq. (61), $H_{m,CDTD}(k)$ is the CDTD channel gain associated with the m-th receive antenna and is given as

$$H_{m,CDTD}(k) = \sum_{n=0}^{N_t-1} \sum_{l=0}^{L-1} h_{m,n,l} \exp\left(-j2\pi k \frac{n\Delta + \tau_l}{N_c}\right). \quad (62)$$

The BER performances of STTD and CDTD are plotted with N_t as a parameter in Fig. 21. A frequency-selective block Rayleigh fading channel having a sample-spaced L = 16-path exponential power delay profile with decay factor β is assumed. Also assumed is that $N_c = 256$, $N_g = 32$,

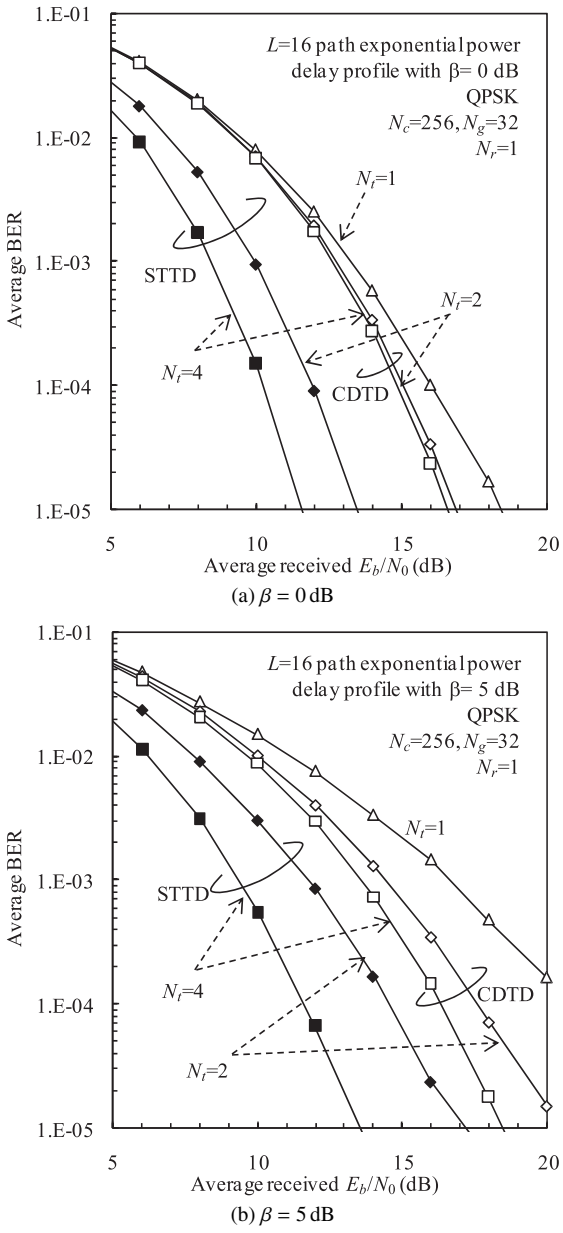

Fig. 21 Performance comparison between STTD and CDTD.

coherent QPSK data-modulation, and ideal channel estimation. The STTD can achieve the N_t-th order diversity irrespective of the channel selectivity, thereby yielding better BER performance than CDTD. CDTD enhances the channel frequency-selectivity to improve the BER performance through MMSE-FDE. However, CDTD is inferior to STTD. The performance degradation of CDTD compared to that for STTD is mainly due to the presence of residual ISI after FDE. The residual ISI cancellation technique can be applied to improve the BER performance of CDTD [62].

8.2 Adaptive Antenna Array (AAA)

In a cellular system, the same carrier frequency is reused in different base stations to utilize efficiently the limited

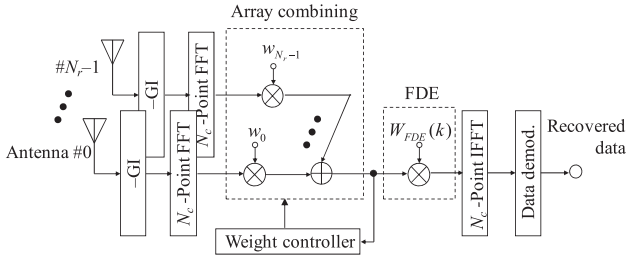

Fig. 22 Receiver structure of frequency-domain AAA using N_r antennas.

spectrum. The presence of co-channel interference (CCI) degrades the transmission performance. The AAA technique [63], [64] can be used to suppress the CCI and increase the received signal-to-interference plus noise power ratio (SINR). AAA using the pre-FFT weight originally proposed for OFDM signal transmission can be applied to SC with FDE [65]. AAA using the pre-FFT is equivalent to an AAA that uses the same array weight for all frequency components in the frequency-domain (this AAA is called the frequency-domain AAA in this paper) and hence, a computationally efficient implementation is possible. The average CCI power minimization criterion is used to determine the array weight in the frequency-domain [66], [67].

Figure 22 illustrates the receiver structure of frequency-domain AAA using N_r antennas. At the receiver, after the removal of the GI, the N_c-point FFT is applied to transform the received signal block into the frequency-domain signal, $\{R_m(k); k = 0 \sim (N_c - 1)\}$, which can be expressed using the matrix form as

$$\begin{aligned}\boldsymbol{R}(k) &= [R_0(k), \cdots, R_m(k), \ldots, R_{N_r-1}(k)]^T \\ &= \sqrt{\frac{2E_s}{T_s}}\boldsymbol{H}(k)S(k) + \boldsymbol{\Pi}(k) + \boldsymbol{N}(k), \end{aligned} \tag{63}$$

where $\boldsymbol{H}(k) = [H_0(k), \ldots, H_m(k), \ldots, H_{Nr-1}(k)]^T$ is the channel gain vector. $\boldsymbol{\Pi}(k)$ and $\boldsymbol{N}(k)$ denote the CCI vector and the noise vector, respectively. Since the same array weight vector, $\boldsymbol{w}_{array} = [w_0, \ldots, w_m, \ldots, w_{Nr-1}]^T$, is used for all frequencies, very fast weight convergence can be achieved even if the simple normalized LMS (NLMS) algorithm [68] is used. The array combiner output $\tilde{R}(k)$, $k = 0 \sim (N_c - 1)$, is given as

$$\tilde{R}(k) = \boldsymbol{w}_{array}^T \boldsymbol{R}(k) \tag{64}$$

with $\|\boldsymbol{w}_{array}\|^2 = 1$, where $\|.\|$ denotes the vector norm. MMSE-FDE is carried out as

$$\hat{R}(k) = W_{FDE}(k)\tilde{R}(k), \tag{65}$$

where $W_{FDE}(k)$ is the MMSE-FDE weight given by

$$W_{FDE}(k) = \frac{\left(\boldsymbol{w}_{array}^T \boldsymbol{H}(k)\right)^*}{|\boldsymbol{w}_{array}^T \boldsymbol{H}(k)|^2 + (E_s/I_0)^{-1}} \tag{66}$$

with I_0 being the average CCI plus noise power spectrum density.

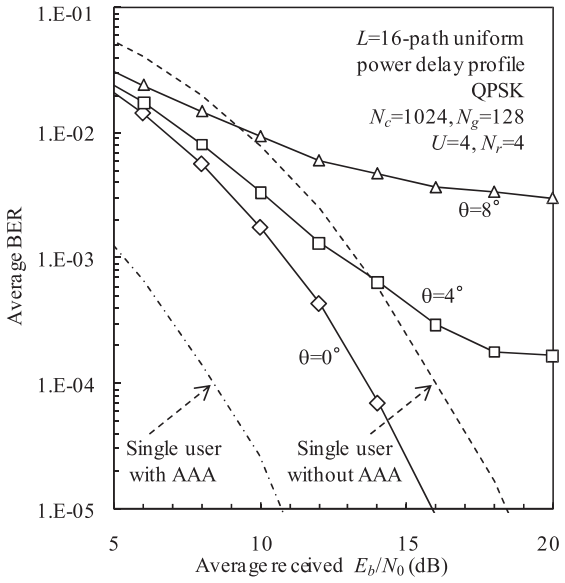

Fig. 23 BER performance of frequency-domain AAA. Single-cell case.

The weight updating can be done in the frequency direction using the NLMS algorithm. The q-th weight updating can be done as

$$\tilde{\boldsymbol{w}}_{array}^{(q)} = \boldsymbol{w}_{array}^{(q-1)} + 2\mu e(k)\frac{\boldsymbol{R}^*(k)}{\|\boldsymbol{R}(k)\|^2} \tag{67}$$

with

$$\boldsymbol{w}_{array}^{(q)} = \frac{\tilde{\boldsymbol{w}}_{array}^{(q)}}{\|\tilde{\boldsymbol{w}}_{array}^{(q)}\|}, \tag{68}$$

where $k = q \bmod N_c$ and $e(k)$ is the error signal between $\tilde{R}(k)$ and the reference signal $\sqrt{2E_s/T_s}\left\{\boldsymbol{w}_{array}^{(q-1)}\right\}^T \boldsymbol{H}(k)P(k)$, and is given by

$$e(k) = \tilde{R}(k) - \sqrt{\frac{2E_s}{T_s}}\left\{\boldsymbol{w}_{array}^{(q-1)}\right\}^T \boldsymbol{H}(k)P(k) \tag{69}$$

with $P(k)$ being the k-th frequency component of the pilot block. Note that $\boldsymbol{w}_{array}$ does not need to track the fading. Tracking against the fading is a task for FDE. Furthermore, the weight updating can be done as many as N_c times during one pilot block. Because of this, very fast weight convergence can be achieved despite using the simple NLMS algorithm.

Figure 23 plots the BER performance of frequency-domain AAA with the arrival angle spread θ (degree) of the propagation paths as a parameter, assuming $N_c = 1024$, $N_r = 4$, and $U = 4$ (4 active users). A single-cell environment is assumed. The directions of the arrival angles (DOAs) of the four users are 60 (desired user), 120, 162, and 330 degrees. When $\theta = 0$, BER performance better than that for the single user case can be obtained due to the array gain. However, as θ increases, the BER performance degrades. This is due to the insufficient degree of freedom of frequency-domain AAA, resulting from the use of the same array weight for all frequency components. This result indicates that the application of frequency-domain AAA is limited to a propagation environment where no major scatterers exist near the receiver, e.g., the uplink signal reception at a high-elevation base station.

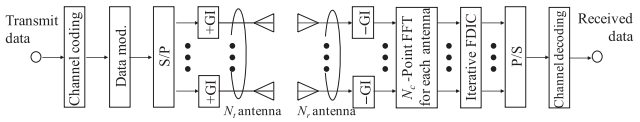

Fig. 24 Transmitter/receiver structure of (N_t, N_r) MIMO SDM.

8.3 MIMO SDM

Although the demand for broadband data services will be high in future wireless communication systems, the available bandwidth is limited. SDM is widely accepted as a promising technique to achieve highly spectrum-efficient signal transmission [52]. In SDM, different data streams are transmitted in parallel from different transmit antennas using the same carrier frequency. At each receive antenna, a superposition of data streams transmitted from different antennas is received. Various signal separation/detection schemes have been proposed such as maximum likelihood detection (MLD) [4], ZF detection [4], MMSE detection [4], and vertical-Bell Laboratories layered space-time architecture (V-BLAST) [69].

The BER performance of SC signal transmission degrades due to the presence of ISI in a strong frequency-selective channel. Therefore, the receiver must perform two tasks: channel equalization and signal separation/detection. In [70], [71], an adaptive MMSE-FDE is presented for SC-MIMO systems. The interference cancellation (IC) technique can provide much improved performance compared to the MMSE-FDE based technique. In [72], two SC-MIMO architectures using IC are proposed. The first architecture combines the conventional FDE with time-domain decision feedback equalization and the second architecture combines FDE with parallel IC (FDE-PIC). The introduction of iterative processing into IC provides much improved performance. The frequency-domain iterative PIC combined with MMSE-FDE is proposed in [73].

Let us consider (N_t, N_r) MIMO SDM using the iterative PIC combined with 2D-MMSE FDE (called iterative FDIC). Figure 24 illustrates the transmitter/receiver structure of (N_t, N_r) SC-MIMO. The data-modulated symbol stream is serial-to-parallel (S/P) converted into N_t parallel streams $\{d_n(t);\ t = 0 \sim (N_c - 1)\}$, $n = 0 \sim (N_t - 1)$. After inserting the CP into the GI, N_t parallel streams are transmitted simultaneously from N_t transmit antennas.

At a receiver, after the removal of the GI, the received signal block $\{r_m(t);\ t = 0 \sim (N_c - 1)\}$ at the m-th ($m = 0 \sim (N_r - 1)$) receive antenna is transformed using the N_c-point FFT into the frequency-domain signal $\{R_m(k);\ k = 0 \sim (N_c - 1)\}$. The frequency-domain received signal vector $\boldsymbol{R}(k) = [R_0(k), \cdots, R_m(k), \cdots, R_{N_r-1}(k)]^T$ is expressed as

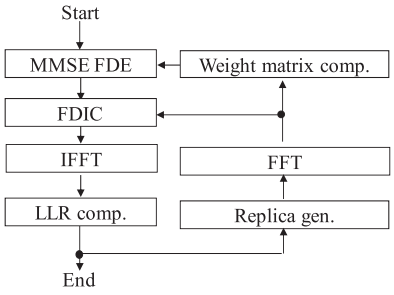

Fig. 25 Iterative FDIC.

$$\boldsymbol{R}(k) = \boldsymbol{H}(k)\boldsymbol{S}(k) + \boldsymbol{N}(k)$$
$$= \sqrt{\frac{2E_s}{T_s}} \begin{bmatrix} H_{0,0}(k) & \cdots & H_{0,N_t-1}(k) \\ & \ddots & \\ \vdots & H_{m,n}(k) & \vdots \\ & & \ddots \\ H_{N_r-1,0}(k) & \cdots & H_{N_r-1,N_t-1}(k) \end{bmatrix}$$
$$\times \begin{bmatrix} S_0(k) \\ \vdots \\ S_n(k) \\ \vdots \\ S_{N_t-1}(k) \end{bmatrix} + \begin{bmatrix} N_0(k) \\ \vdots \\ N_m(k) \\ \vdots \\ N_{N_r-1}(k) \end{bmatrix}, \quad (70)$$

where $\boldsymbol{H}(k)$ is an $N_r \times N_t$ channel matrix, $\boldsymbol{S}(k)$ is an $N_t \times 1$ signal vector that has been transmitted from the N_t transmit antennas, and $\boldsymbol{N}(k)$ is an $N_t \times 1$ noise vector. At the i-th iteration stage in iterative FDIC (see Fig. 25), MMSE-FDE is first carried out as

$$\hat{\boldsymbol{R}}^{(i)}(k) = \{\boldsymbol{W}^{(i)}(k)\}^T \boldsymbol{R}(k) \quad (71)$$

to suppress the inter-antenna interference (IAI) and ISI simultaneously, where $\boldsymbol{W}^{(i)}(k)$ is an $N_r \times N_t$ MMSE weight matrix. Its n-th ($n = 0 \sim (N_t - 1)$) column vector $\boldsymbol{W}_n^{(i)}(k)$ is given as

$$\boldsymbol{W}_n^{(i)}(k) = \boldsymbol{H}_n^H(k)\left[\boldsymbol{H}(k)\boldsymbol{G}_n^{(i)}(k)\boldsymbol{H}^H(k) + (E_s/N_0)^{-1}\boldsymbol{I}\right]^{-1}, \quad (72)$$

where $\boldsymbol{I}$ is an $N_r \times N_r$ identity matrix, $\boldsymbol{H}_n(k)$ is the n-th column vector of $N_r \times N_t$ channel gain matrix $\boldsymbol{H}(k)$, and $\boldsymbol{G}_n^{(i)}(k) = \mathrm{diag}\{g_0^{(i)}(k), \cdots, g_{n'}^{(i)}(k), \cdots, g_{N_t-1}^{(i)}(k)\}$ with $g_{n'}^{(i)}(k)$ reflecting the interference from the n'-th antenna ($n' = 0 \sim (N_t - 1)$). Note that $g_{n'}^{(i)}(k)$ corresponds to the residual ISI and IAI when $n' = n$ and $n' \neq n$, respectively.

The residual IAI and ISI replicas are generated by feeding back the signal block replicas, $\{\tilde{S}_n^{(i-1)}(k)\}$, $n = 0 \sim (N_t - 1)$, obtained from the $(i-1)$-th iteration and are subtracted from $\hat{R}_n^{(i)}(k)$ as

$$\tilde{R}_n^{(i)}(k) = \hat{R}_n^{(i)}(k) - \sum_{n'=0}^{N_t-1} \tilde{M}_{n'}^{(i)}(k), \quad (73)$$

where $\tilde{M}_{n'}^{(i)}(k)$ is the IAI or ISI replica given by

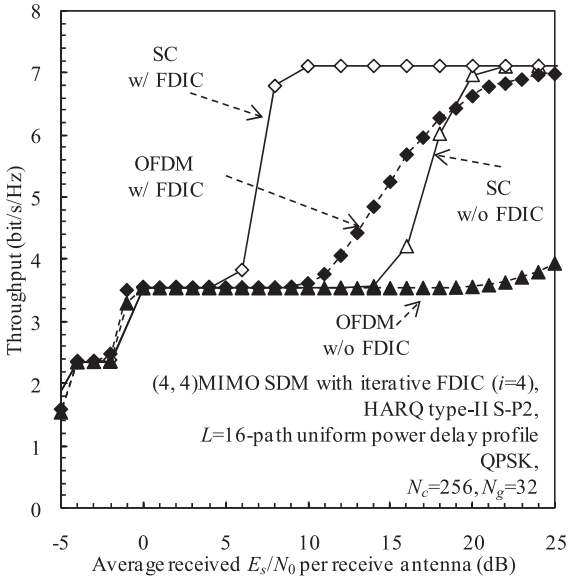

Fig. 26 Throughput performance of (4,4) MIMO SDM with iterative FDIC.

$$\tilde{M}_{n'}^{(i)}(k) = \begin{cases} \sqrt{\frac{2E_s}{T_s}} \hat{H}_{n'}^{(i)}(k) S_{n'}^{(i-1)}(k), & \text{if } n' \neq n \\ \sqrt{\frac{2E_s}{T_s}} \left\{\hat{H}_n^{(i)}(k) - A_n^{(i)}\right\} S_n^{(i-1)}(k), & \text{if } n' = n \end{cases} \quad (74)$$

with

$$\begin{cases} A_n^{(i)} = \dfrac{1}{N_c} \displaystyle\sum_{k=0}^{N_c-1} \left\{\boldsymbol{W}_n^{(i)}(k)\right\}^T \boldsymbol{H}_n(k) \\ \hat{H}_{n'}^{(i)}(k) = \left\{\boldsymbol{W}_{n'}^{(i)}(k)\right\}^T \boldsymbol{H}_{n'}(k) \end{cases} \quad (75)$$

The LLR for each transmitted bit is computed [73], from which the signal block replicas, $\{\tilde{S}_n^{(i)}(k);\ \mathrm{k} = 0 \sim (N_c - 1)\}$, $n = 0 \sim (N_t - 1)$, are generated for the next iteration. The above operations are repeated a sufficient number of times to suppress sufficiently the IAI and ISI.

The HARQ throughput performance of (4,4)MIMO SDM with iterative FDIC ($i = 4$) is plotted in Fig. 26 as a function of the average received E_s/N_0 per receive antenna. $N_r \times N_t$ channels are independent Rayleigh fading channels having an $L = 16$-path uniform power delay profile. Iterative FDIC significantly improves the throughput performance.

In the above iterative FDIC, equalization/interference cancellation is done in an iterative fashion within each received signal block. However, according to the turbo equalization principle [26], the above iterative FDIC can be incorporated into the HARQ processing to achieve higher throughput by iteratively performing joint equalization, interference cancellation, and channel decoding.

9. Frequency-Domain Pre-Equalization

The use of FDE at a receiver (called FDE reception) is an effective technique for improving the SC signal transmission

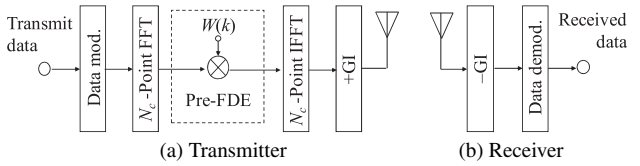

Fig. 27 Transmitter/receiver structures of SC with pre-FDE.

performance in a frequency-selective channel [11]. Another FDE technique is frequency-domain pre-equalization (pre-FDE) transmission [74], [75]. References [76] and [77] introduce pre-FDE into the SC signal transmission. Pre-FDE can be combined with MIMO-SDM [78], [79].

Figure 27 shows the transmitter/receiver structure of SC with pre-FDE [76], [77]. Both pre-FDE for the transmission and FDE for the reception can be implemented at the base station to alleviate the complexity problem of mobile terminals. To perform pre-FDE, the channel state information (CSI) is necessary at the transmitter. Assuming a time division duplex (TDD) system [80], the same carrier frequency is used for both transmit and receive channels; therefore, the channel estimate for FDE reception can be reused for pre-FDE transmission.

Pre-FDE transmission requires FFT and IFFT operations at the transmitter. The N_c-point FFT is applied to transform the transmit symbol vector $\boldsymbol{s} = [s(0), \ldots, s(k), \ldots, s(N_c-1)]^T$ into the frequency-domain transmit signal vector $\boldsymbol{S} = [S(0), \ldots, S(k), \ldots, S(N_c-1)]^T$. After multiplying the complex-valued weight matrix $\boldsymbol{W} = \mathrm{diag}\{W(0), \ldots, W(k), \ldots, W(N_c-1)\}$, the pre-equalized time-domain signal vector $\boldsymbol{s}_{pre-FDE}$ is obtained using the N_c-point IFFT as

$$\boldsymbol{s}_{pre-FDE} = \sqrt{\frac{2E_s}{T_s}} C \cdot \boldsymbol{F}^H \boldsymbol{W} \boldsymbol{S}, \tag{76}$$

where $\boldsymbol{F}$ is an $N_c \times N_c$ FFT matrix, $\boldsymbol{S} = \boldsymbol{F}\boldsymbol{s}$, and $C = \|\boldsymbol{W}\boldsymbol{S}\|^{-1} = \left(\sum_{k=0}^{N_c-1} |W(k)S(k)|^2\right)^{-1/2}$ is the transmit power normalization factor so as to always keep the block averaged transmit powers after and before pre-FDE the same. Using the MMSE weight matrix, the k-th element, $W(k)$, of $\boldsymbol{W}$ is given by [77]

$$W(k) = \frac{H^*(k)}{|H(k)|^2 + (E_s/N_0)^{-1}}. \tag{77}$$

After inserting the CP into the GI, the pre-equalized signal is transmitted over a frequency-selective channel. The received signal vector, $\boldsymbol{r} = [r(0), \ldots, r(t), \ldots, r(N_c-1)]^T$, after removal of the GI is given as

$$\boldsymbol{r} = \boldsymbol{h}\boldsymbol{s}_{pre-FDE} + \boldsymbol{n}, \tag{78}$$

where $\boldsymbol{h}$ is the circulant channel impulse response matrix given by Eq. (6) and $\boldsymbol{n}$ is the $N_c \times 1$ noise vector.

Since $\boldsymbol{h} = \boldsymbol{F}^H \boldsymbol{H} \boldsymbol{F}$, Eq. (78) can be rewritten as

$$\begin{aligned} \boldsymbol{r} &= \boldsymbol{F}^H \boldsymbol{H} \boldsymbol{F} \boldsymbol{s}_{pre-FDE} + \boldsymbol{n} \\ &= \sqrt{\frac{2E_s}{T_s}} C \cdot \boldsymbol{F}^H \boldsymbol{H} \boldsymbol{W} \boldsymbol{F} \boldsymbol{s} + \boldsymbol{n}. \end{aligned} \tag{79}$$

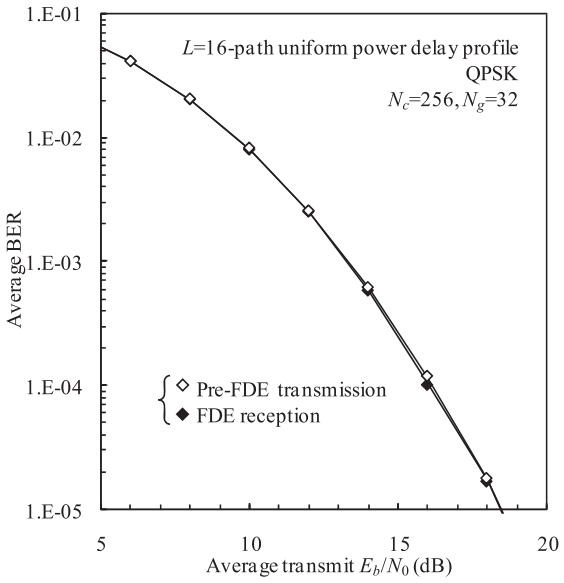

Fig. 28 Performance comparison between pre-FDE transmission and FDE reception.

Similar to Eq. (20), Eq. (78) can be further rewritten as

$$\boldsymbol{r} = \sqrt{\frac{2E_s}{T_s}} C \cdot A \cdot \boldsymbol{s} + \boldsymbol{F}^H \boldsymbol{M} + \boldsymbol{n}, \tag{80}$$

where A is the average equivalent channel gain and $\boldsymbol{M}$ is the frequency-domain residual ISI vector of size $N_c \times 1$ and they are given as

$$\begin{cases} A = \dfrac{1}{N_c} \displaystyle\sum_{k=0}^{N_c-1} H(k)W(k) \\ \boldsymbol{M} = \sqrt{\dfrac{2E_s}{T_s}} C \left(\boldsymbol{H}\boldsymbol{W} - A \cdot \boldsymbol{I}\right) \boldsymbol{F}\boldsymbol{s} \end{cases}. \tag{81}$$

Therefore, the received signal vector $\boldsymbol{r}$ can be the estimate $\hat{\boldsymbol{s}}$ of the transmitted symbol vector $\boldsymbol{s}$. Comparison of Eqs. (20) and (80) shows that pre-FDE transmission provides the desired signal component and residual ISI identical to the FDE reception.

The BER performance of pre-FDE transmission and FDE reception are compared in Fig. 28. We assume $N_c = 256$, $N_g = 32$, QPSK data-modulation, and frequency-selective block Rayleigh fading channel with a sample-spaced $L = 16$-path uniform power delay profile. Channel estimation is assumed to be ideal. The figure shows that pre-FDE transmission and FDE reception provide the identical performance. This clearly illustrates the potential of pre-FDE transmission for its application to the downlink (base-to-mobile).

10. Conclusion

In future wireless communication systems, broadband data services will be in demand and the wireless channel will

become severely frequency-selective. Therefore, the multi-carrier (MC) transmission technique has been attracting much attention. However, it has been proven that the single-carrier (SC) signal transmission with frequency-domain equalization (FDE) can provide very attractive transmission performance. Many investigations have been done on SC with FDE. In this article, we reviewed SC with FDE. The principle of simple one-tap FDE, residual ISI cancellation, channel estimation, and MIMO technique were introduced. Both MC and SC signal transmission techniques can be applied to future wireless communication systems.

Broadband data transmission requires prohibitively high transmit powers from mobile terminals. This cannot be allowed in practical systems. The power problem is an important issue to address as well as the frequency-selective channel problem in order to achieve frequency and power efficient future wireless communication systems. Many interesting research topics remain regarding SC with FDE. They include distributed antenna technique and multihop relaying to reduce the transmit power while achieving frequency diversity gain through the simple one-tap FDE.

References

[1] F. Adachi, M. Sawahashi, and H. Suda, "Wideband DS-CDMA for next generation mobile communications systems," IEEE Commun. Mag., vol.36, no.9, pp.56–69, Sept. 1998.
[2] H. Ekström, A. Furuskär, J. Karlsson, M. Meyer, S. Parkvall, J. Torsner, and M. Wahlqvist, "Technical solutions for the 3G long-term evolution," IEEE Commun. Mag., vol.44, no.3, pp.38–45, March 2006.
[3] Y. Kim, B.J. Jeong, J. Chung, C.-S. Hwang, J.S. Ryu, K.-H. Kim, and Y.J. Kim, "Beyond 3G; vision, requirements, and enabling technologies," IEEE Commun. Mag., vol.41, no.3, pp.120–124, March 2003.
[4] J.G. Proakis, Digital Communications, 4th ed., McGraw-Hill, 2001.
[5] S. Hara and R. Prasad, "Overview of multicarrier CDMA," IEEE Commun. Mag., vol.35, no.12, pp.126–133, Dec. 1997.
[6] N. Yee, J.P. Linnartz, and G. Fettweis, "Multi-carrier CDMA in indoor wireless radio networks," IEICE Trans. Commun., vol.E77-B, no.7, pp.900–904, July 1994.
[7] E.A. Sourour and M. Nakagawa, "Performance of orthogonal multicarrier CDMA in a multipath fading channel," IEEE Trans. Commun., vol.44, no.3, pp.356–367, March 1996.
[8] H. Sari, G. Karam, and I. Jeanclaude, "An analysis of orthogonal frequency-division multiplexing for mobile radio applications," Proc. IEEE VTC 1994, vol.3, pp.1635–1639, June 1994.
[9] H. Sari, G. Karam, and I. Jeanclaude, "Transmission techniques for digital terrestrial TV broadcasting," IEEE Commun. Mag., vol.33, no.2, pp.100–109, Feb. 1995.
[10] A. Czylwik, "Comparison between adaptive OFDM and single carrier modulation with frequency domain equalization," Proc. IEEE VTC 1997-Spring, vol.2, pp.865–869, Phoenix, Ariz, U.S.A., May 1997.
[11] D. Falconer, S.L. Ariyavistakul, A. Benyamin-Seeyar, and B. Eidson, "Frequency domain equalization for single-carrier broadband wireless systems," IEEE Commun. Mag., vol.40, no.4, pp.58–66, April 2002.
[12] A.S. Madhukumar, F. Chin, Y.-C. Liang, and K. Yang, "Single-carrier cyclic prefix-assisted CDMA system with frequency domain equalization for high data rate transmission," EURASIP Journal on Wireless Communications and Networking, vol.2004, no.1, pp.149–160, Aug. 2004.
[13] F. Adachi, D. Garg, S. Takaoka, and K. Takeda, "Broadband CDMA techniques," IEEE Wireless Commun. Mag., vol.12, no.2, pp.8–18, April 2005.
[14] H.G. Myung, J. Lim, and D.J. Goodman, "Single carrier FDMA for uplink wireless transmission," IEEE Vehicular Technol. Mag., vol.1, no.3, pp.30–38, Sept. 2006.
[15] T.S. Rappaport, Wireless Communications, Prentice Hall, 1996.
[16] C.A. Belfiore and J.H. Park, Jr., "Decision-feedback equalization," Proc. IEEE, vol.67, pp.1143–1156, Aug. 1979.
[17] M.E. Austin, "Decision-feedback equalization for digital communication over dispersive channels," M.I.T. Res. Lab. Electron., Tech. Rep., 461, Aug. 1967.
[18] O. Monsen, "Feedback equalization for fading dispersive channels," IEEE Trans. Inf. Theory, vol.17, no.1, pp.56–64, Jan. 1971.
[19] J. Salz, "Optimum mean square decision feedback equalization," Bell Syst. Tech. J., vol.52, pp.1341–1373, Oct. 1973.
[20] D. Falconer and J. Foschini, "Theory of minimum mean square error Q.A.M. system employing decision feedback equalization," Bell Syst. Tech. J., vol.52, pp.1821–1849, Oct. 1973.
[21] A.M. Chan and G.W. Wornell, "A class of block-iterative equalizers for intersymbol interference channels: Fixed channel results," IEEE Trans. Commun., vol.49, no.11, pp.1966–1976, Nov. 2001.
[22] N. Benvenuto and S. Tomasin, "On the comparison between OFDM and single carrier modulation with a DFE using a frequency-domain feedforward filter," IEEE Trans. Commun., vol.50, no.6, pp.947–955, June 2002.
[23] K. Berberidis and J. Palicot, "A frequency domain decision feedback equalizer for multipath echo cancellation," Proc. IEEE GLOBECOM 1995, vol.1, pp.98–102, Singapore, Nov. 1995.
[24] N. Benvenuto and S. Tomasin, "Block iterative DFE for single carrier modulation," Electron. Lett., vol.38, no.19, pp.1144–1145, Sept. 2002.
[25] S. Tomasin and N. Benvenuto, "Iterative design and detection of a DFE in the frequency domain," IEEE Trans. Commun., vol.53, no.11, pp.1867–1875, Nov. 2005.
[26] R. Koetter, A.C. Singer, and M. Tuchler, "Turbo equalization," IEEE Signal Process. Mag., vol.21, no.1, pp.67–80, Jan. 2004.
[27] W. Shiech, X. Yi, Y. Ma, and Q. Yang, "Coherent optical OFDM: Has its time come?," Journal of Optical Networking, vol.7, no.3, pp.234–255, March 2008.
[28] K. Ishihara, T. Kobayashi, R. Kudo, Y. Takatori, A. Sano, E. Yamada, H. Masuda, and Y. Miyamoto, "Frequency-domain equalization for optical transmission systems," Electron. Lett., vol.44, no.14, pp.870–871, July 2008.
[29] J. Louveaux, L. Vandendorpe, and T. Sartenaer, "Cyclic prefixed single carrier and multicarrier transmission: Bit rate comparison," IEEE Commun. Lett., vol.7, no.4, pp.180–182, April 2003.
[30] I.S. Gradshteyn and I.M. Ryzhik, Table of integrals, series, and products, Academic Press, New York, 1965.
[31] T. Shi, S. Zhou, and Y. Yao, "Capacity of single carrier systems with frequency-domain equalization," Proc. IEEE Circuits and Systems Symposium on Emerging Technologies, vol.2, pp.429–432, June 2004.
[32] J.J. Shynk, "Frequency-domain and multirate adaptive filtering," IEEE Signal Process. Mag., vol.9, no.1, pp.14–37, Jan. 1992.
[33] D. Falconer and S.L. Ariyavisitakul, "Broadband wireless using single carrier and frequency domain equalization," Proc. 5th International Symposium on Wireless Personal Multimedia Communications (WPMC), vol.1, pp.27–36, Oct. 2002.
[34] I. Martoyo, T. Weiss, F. Capar, and F.K. Jondral, "Low complexity CDMA downlink receiver based on frequency domain equalization," Proc. IEEE VTC 2003-Fall, vol.2, pp.987–991, Orland, FL, U.S.A., Oct. 2003.
[35] K. Takeda, H. Tomeba, and F. Adachi, "Iterative overlap FDE for DS-CDMA without GI," Proc. IEEE VTC 2006-Fall, Montreal, Quebec, Canada, Sept. 2006.
[36] K. Takeda, H. Tomeba, K. Takeda, and F. Adachi, "DS-CDMA

HARQ with overlap FDE," IEICE Trans. Commun., vol.E90-B, no.11, pp.3189–3196, Nov. 2007.
[37] K. Takeda, T. Obara, H. Tomeba, and F. Adachi, "Throughput comparison of single-carrier and multi-carrier signal transmissions using overlap FDE," IEICE Technical Report, RCS2008-169, Nov. 2008.
[38] D. Garg and F. Adachi, "Throughput comparison of turbo-coded HARQ in OFDM, MC-CDMA and DS-CDMA with frequency-domain equalization," IEICE Trans. Commun., vol.E88-B, no.2, pp.664–677, Feb. 2005.
[39] C. Tepedelenlioglu and R. Challagulla, "Low-complexity multipath diversity through fractional sampling in OFDM," IEEE Trans. Signal Process., vol.52, no.11, pp.3104–3116, Nov. 2004.
[40] P.P. Vaidyanathan and B. Vrcelj, "Theory of fractionally spaced cyclic-prefix equalizers," Proc. IEEE International Conference on Acoustics, Speech, and Signal Processing (ICASSP), vol.2, pp.1277–1280, Orlando, FL, U.S.A., May 2002.
[41] Y. Yoshida, K. Hayashi, and H. Sakai, "Pre- and post-equalization and frequency diversity combining methods for block transmission with cyclic prefix," IEICE Trans. Commun., vol.E90-B, no.10, pp.2874–2883, Oct. 2007.
[42] K. Takeda and F. Adachi, "Frequency-domain interchip interference cancellation for DS-CDMA downlink transmission," IEEE Trans. Veh. Technol., vol.56, no.3, pp.1286–1294, May 2007.
[43] F. Adachi, K. Takeda, and Y. Kojima, "On computation of mean squared equalization error for single-carrier iterative frequency-domain equalization & residual interference cancellation," Proc. IEICE Gen. Conf. 2009, March 2009.
[44] J.-J. van de Beek, O. Edfors, M. Sandell, S.K. Wilson, and P.O. Borjesson, "On channel estimation in OFDM systems," Proc. IEEE VTC 1995, pp.815–819, Chicago, IL, July 1995.
[45] P. Hoeher, S. Kaiser, and P. Robertson, "Pilot-symbol-aided channel estimation in time and frequency," Proc. IEEE GLOBECOM 1997, pp.90–96, Nov. 1997.
[46] D.C. Chu, "Polyphase codes with good periodic correlation properties," IEEE Trans. Inf. Theory, vol.18, no.4, pp.531–532, July 1972.
[47] M. Morelli, L. Sanguinetti, and U. Mengali, "Channel estimation for adaptive frequency-domain equalization," IEEE Trans. Wireless Commun., vol.4, no.5, pp.2508–2518, Sept. 2005.
[48] Y. Wang and X. Dong, "Frequency-domain channel estimation for SC-FDE in UWB communications," IEEE Trans. Commun., vol.54, no.12, pp.2155–2163, Dec. 2006.
[49] K. Takeda and F. Adachi, "Frequency-domain MMSE channel estimation for frequency-domain equalization of DS-CDMA signals," IEICE Trans. Commun., vol.E90-B, no.7, pp.1746–1753, July 2007.
[50] Y. Zeng and T.S. Ng, "Pilot cyclic prefixed single carrier communication: Channel estimation and equalization," IEEE Signal Process. Lett., vol.12, no.1, pp.56–59, Jan. 2005.
[51] K. Ishihara, K. Takeda, and F. Adachi, "Iterative channel estimation for frequency-domain equalization of DSSS signals," IEICE Trans. Commun., vol.E90-B, no.5, pp.1171–1180, May 2007.
[52] G.J. Foschini and M.J. Gans, "On limits of wireless communications in a fading environment when using multiple antennas," Wirel. Pers. Commun., vol.6, no.3, pp.311–335, 1998.
[53] F.W. Vook, T.A. Thomas, and K.L. Baum, "Cyclic-prefix CDMA with antenna diversity," Proc. IEEE VTC 2002-Spring, vol.2, pp.1002–1006, May 2002.
[54] F. Adachi and K. Takeda, "Bit error rate analysis of DS-CDMA with joint frequency-domain equalization and antenna diversity combining," IEICE Trans. Commun., vol.E87-B, no.10, pp.2991–3002, Oct. 2004.
[55] S. Alamouti, "A simple transmit diversity technique for wireless communications," IEEE J. Sel. Areas Commun., vol.16, no.8, pp.1451–1458, Oct. 1998.
[56] A. Dammann and S. Kaiser, "Standard conformable antenna diversity techniques for OFDM and its application to the DVB-T system," Proc. IEEE GLOBECOM 2001, vol.4, pp.3100–3105, Nov. 2001.
[57] A. Lodhi, F. Said, M. Dohler, and A.H. Aghvami, "Performance comparison of space-time block coded and cyclic delay diversity MC-CDMA systems," IEEE Trans. Wireless Commun., vol.12, no.2, pp.38–45, April 2005.
[58] N. Al-Dhahir, "Single-carrier frequency-domain equalization for space-time block coded transmissions over frequency-selective fading channels," IEEE Commun. Lett., vol.5, no.7, pp.304–306, July 2001.
[59] K. Takeda, T. Itagaki, and F. Adachi, "Application of space-time transmit diversity to single-carrier transmission with frequency-domain equalization and receive antenna diversity in a frequency-selective fading channel," IEE Proc. Communications, vol.151, no.6, pp.627–632, Dec. 2004.
[60] R. Kawauchi, K. Takeda, and F. Adachi, "Space-time cyclic delay transmit diversity for a multi-code DS-CDMA signal with frequency-domain equalization," IEICE Trans. Commun., vol.E90-B, no.3, pp.591–596, March 2007.
[61] Y.-C. Liang, W.S. Leon, Y. Zenq, and C. Xu, "Design of cyclic delay diversity for single carrier cyclic prefix (SCCP) transmissions with block-iterative GDFE (BI-GDFE) receiver," IEEE Trans. Wireless Commun., vol.7, no.2, pp.677–684, Feb. 2008.
[62] K. Takeda, Y. Kojima, and F. Adachi, "Transmit diversity for DS-CDMA/MMSE-FDE with frequency-domain ICI cancellation," Proc. IEEE VTC 2008-Spring, pp.1057–1061, May 2008.
[63] L.C. Godara, "Application of antenna arrays to mobile communications, Part I: Performance improvement, feasibility, and system considerations," Proc. IEEE, vol.85, no.7, pp.1029–1060, July 1997.
[64] L.C. Godara, "Application of antenna arrays to mobile communications, Part II: Beam-forming and direction of arrival consideration," Proc. IEEE, vol.85, no.8, pp.1195–1245, Aug. 1997.
[65] K. Hayashi, T. Kojima, and H. Sakai, "An adaptive antenna array for single carrier modulation system with cyclic prefix," Proc. IEEE VTC 2003-Spring, vol.2, pp.1015–1019, April 2003.
[66] K. Takeda, R. Kawauchi, and F. Adachi, "Frequency-domain adaptive antenna array for single-carrier uplink transmission using frequency-domain equalization," Proc. 9th WPMC, pp.776–780, San Diego, U.S.A., Sept. 2006.
[67] B.-W. Kang, K. Takeda, and F. Adachi, "Performance of single-carrier frequency-domain adaptive antenna array," Proc. IEEE VTC 2007-Fall, Baltimore, USA, Sept.-Oct. 2007.
[68] S. Haykin, Adaptive Filter Theory, 4th ed., Prentice Hall, 2001.
[69] P.W. Wolniansky, G.J. Foschini, G.D. Golden, and R.A. Valenzuela, "V-BLAST: An architecture for realizing very high data rates over the rich-scattering wireless channel," Proc. International Symposium on Signals, Systems, and Electronics, pp.295–300, Sept. 1998.
[70] J. Coon, S. Armour, M. Beach, and J. McGeehan, "Adaptive frequency-domain equalization for single-carrier multiple-input multiple-output wireless transmissions," IEEE Trans. Signal Process., vol.53, no.8, pp.3247–3256, Aug. 2005.
[71] J. Coon, S. Armour, M. Beach, and J. McGeehan, "Adaptive frequency-domain equalization for single-carrier MIMO systems," Proc. IEEE International Conference on Communications (ICC), vol.4, pp.2487–2491, June 2004.
[72] X. Zhu and R.D. Murch, "Novel frequency-domain equalization architectures for a single-carrier wireless MIMO system," Proc. IEEE VTC2002-Fall, vol.2, pp.874–878, Sept. 2002.
[73] A. Nakajima and F. Adachi, "Iterative FDIC using 2D-MMSE FDE for turbo-coded HARQ in SC-MIMO multiplexing," IEICE Trans. Commun., vol.E90-B, no.3, pp.693–695, March 2007.
[74] D. Mottier and D. Castelain, "SINR-based channel pre-equalization for uplink multi-carrier CDMA systems," Proc. IEEE PIMRC, vol.4, pp.1488–1492, Sept. 2002.
[75] I. Cosovic, M. Schnell, and A. Springer, "On the performance of different channel pre-compensation techniques for uplink time division duplex MC-CDMA," Proc. IEEE VTC 2003-Fall, Oct. 2003.
[76] L.-U Choi and R. Murch, "Frequency domain pre-equalization with transmit diversity for MISO broadband wireless communications," Proc. IEEE VTC 2002-Fall, vol.3, pp.1787–1791, Sept. 2002.

[77] F. Adachi, K. Takeda, and H. Tomeba, "Frequency-domain pre-equalization for multicode direct sequence spread spectrum signal transmission," IEICE Trans. Commun., vol.E88-B, no.7, pp.3078–3081, July 2005.
[78] L.-U Choi and R. Murch, "A transmit MIMO scheme with frequency domain pre-equalization for wireless frequency selective channels," IEEE Trans. Wireless Commun., vol.3, no.3, pp.929–938, May 2004.
[79] L.-U Choi and R. Murch, "A pre-BLAST-DFE technique for the downlink of frequency-selective fading MIMO channels," IEEE Trans. Commun., vol.52, no.5, pp.737–743, May 2004.
[80] R. Esmailzadeh, M. Nakagawa, and A. Jones, "TDD-CDMA for the 4th generation of wireless communications," IEEE Wireless Commun. Mag., vol.10, no.4, pp.8–15, Aug. 2003.

Fumiyuki Adachi received the B.S. and Dr. Eng. degrees in electrical engineering from Tohoku University, Sendai, Japan, in 1973 and 1984, respectively. In April 1973, he joined the Electrical Communications Laboratories of Nippon Telegraph & Telephone Corporation (now NTT) and conducted various types of research related to digital cellular mobile communications. From July 1992 to December 1999, he was with NTT Mobile Communications Network, Inc. (now NTT DoCoMo, Inc.), where he led a research group on wideband/broadband CDMA wireless access for IMT-2000 and beyond. Since January 2000, he has been with Tohoku University, Sendai, Japan, where he is a Professor of Electrical and Communication Engineering at the Graduate School of Engineering. His research interests are in CDMA wireless access techniques, equalization, transmit/receive antenna diversity, MIMO, adaptive transmission, and channel coding, with particular application to broadband wireless communications systems. From October 1984 to September 1985, he was a United Kingdom SERC Visiting Research Fellow in the Department of Electrical Engineering and Electronics at Liverpool University. He was a co-recipient of the IEICE Transactions best paper of the year award 1996 and again 1998 and also a recipient of Achievement award 2003. He is an IEEE Fellow and was a co-recipient of the IEEE Vehicular Technology Transactions best paper of the year award 1980 and again 1990 and also a recipient of Avant Garde award 2000. He was a recipient of the Thomson Scientific Research Front Award 2004 and the Ericsson Telecommunications Award 2008.

Hiromichi Tomeba received his B.S., M.S., and Dr. Eng. degrees in communications engineering from Tohoku University, Sendai, Japan, in 2004, 2006, and 2008, respectively. Since 2006, he has been a Japan Society for the Promotion of Science (JSPS) research fellow. Currently he is a JSPS postdoctoral fellow at the Department of Electrical and Communications Engineering, Graduate School of Engineering, Tohoku University. His research interests include frequency-domain equalization and antenna diversity techniques for mobile communication systems. He was a recipient of the IEICE RCS (Radio Communication Systems) Active Research Award in 2004 and 2005.

Kazuki Takeda received his B.S. and M.S. degrees in communications engineering from Tohoku University, Sendai, Japan, in 2006 and 2008. Currently he is a Japan Society for the Promotion of Science (JSPS) research fellow, studying toward his PhD degree at the Department of Electrical and Communications Engineering, Graduate School of Engineering, Tohoku University. His research interests include precoding and channel equalization techniques for mobile communication systems.